Minor Bodies

in the Planetary System

Hermann Boehnhardt

MPI for Solar System Research

Katlenburg-Lindau

Asteroids

- **Summary**
  - Asteroids = remnants from formation disk between Mars and Jupiter
  - irregular shape except large ones
  - Did not make it to form a planet (Jupiter influence)
  - Continuous loss of asteroids from belt
  - Kirkwood gaps = gravitational scattering by Jupiter
  - Hirayama families = collision groups
  - Taxonomy classes = differentiated bodies
  - Solar distance distribution of taxonomic classes with signature from formation period

Orbits

- **Asteroid belt:**
  - largest concentration between Mars and Jupiter
  - much lower at other (larger&smaller) distances
  - within asteroid belts gaps with low number density

    ➔ Kirkwood gaps
  - Gaps are located at integer-ratio resonances between asteroid and Jupiter revolution periods

    Resonance effects: Jupiter increases eccentricity of asteroids when in resonance orbit, short life time of objects in resonance orbits

    ➔ asteroid becomes planet crossing and is at high risk to collide with terrestrial planets

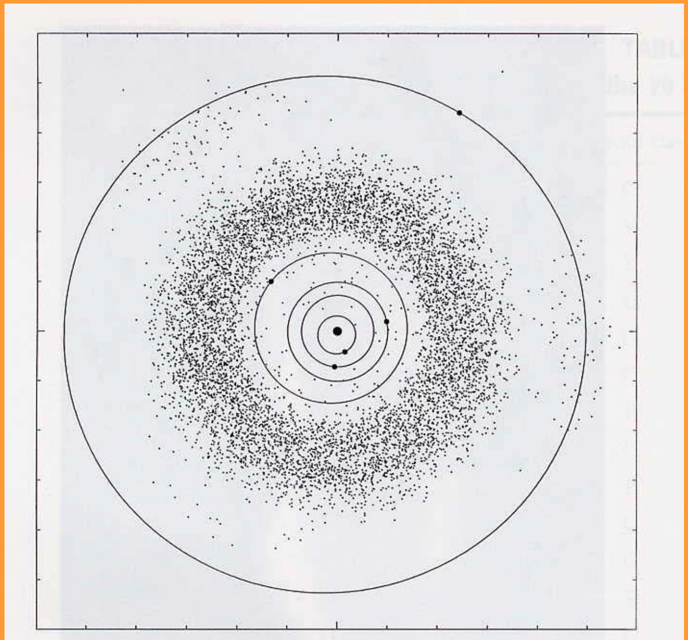

FIGURE 3 Positions projected onto the ecliptic plane for October 4, 2000 of the planets Mercury through Jupiter and 7722 numbered asteroids with accurately known orbits. (Copyright 1998 Institute for Remote Exploration.)

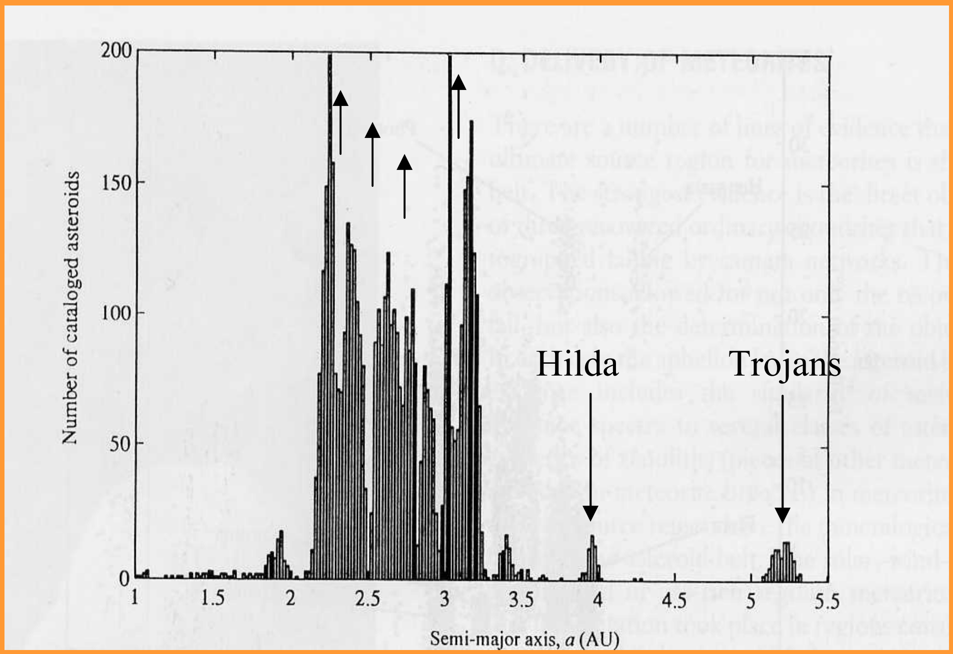

- **Collision families:**
  - Clustering of asteroid orbits with certain orbital parameters
    (a,i) or (a,e) groups
    ➔ Hirayama families
  - Collision families
  - Family members may have different taxonomic properties since they can originate from different part of possibly differentiated bodies by the collision event (for instance from the crust - S-type, from the core – M type)
- **Double asteroids:**
  - Double asteroids exist
    (first discovery: Ida+Dactyl discovered by GALILEO probe during flyby)
  - Formation through impact (?)
    through rotational break-up
    (small ones only)

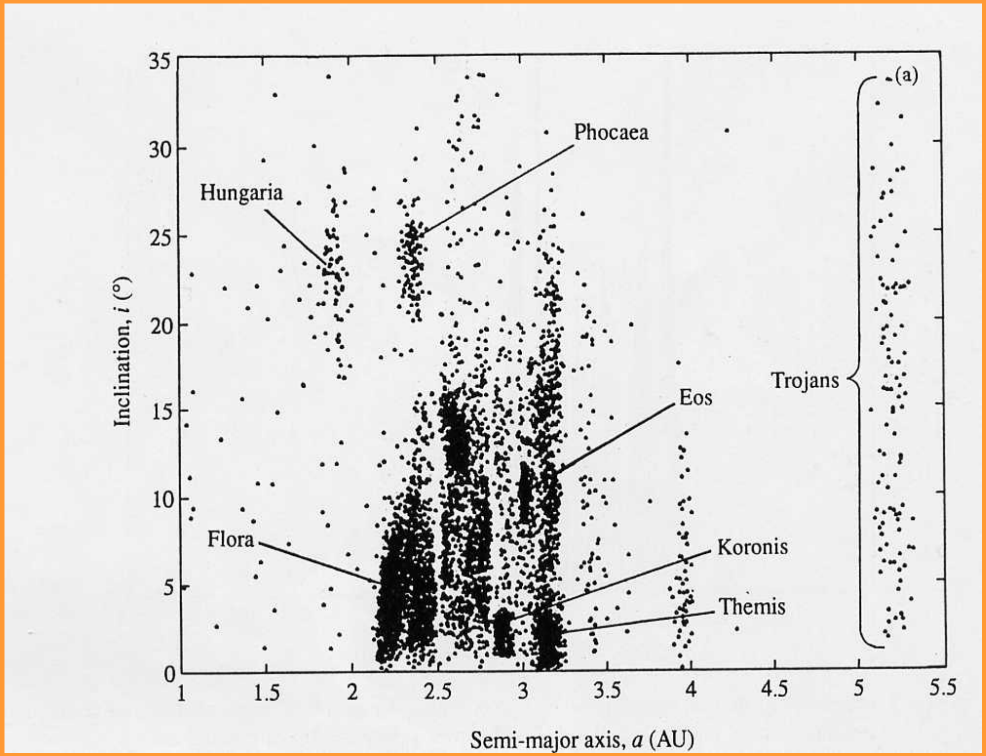

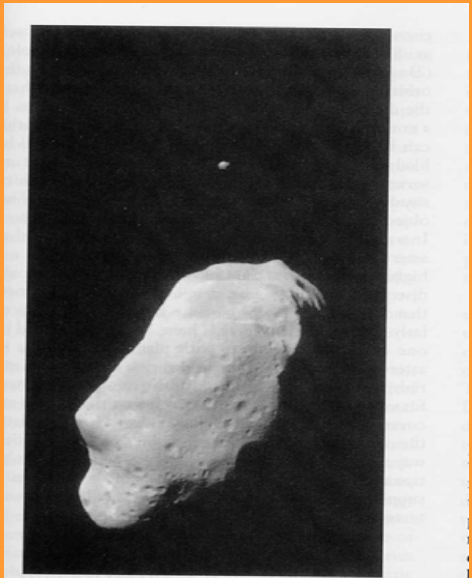

FIGURE 6 243 Ida and its satellite, Dactyl. (Courtesy of NASA/JPL/Caltech.)

Reflectance spectroscopy

Recipe:

- take object spectrum
- take solar analogue spectrum
- divide the two spectra

➔ intrinsic spectrum of the object

solar = flat without slope

gradient = diverse object continuum

absorption/emission = object specific materials

(works also for photometry)

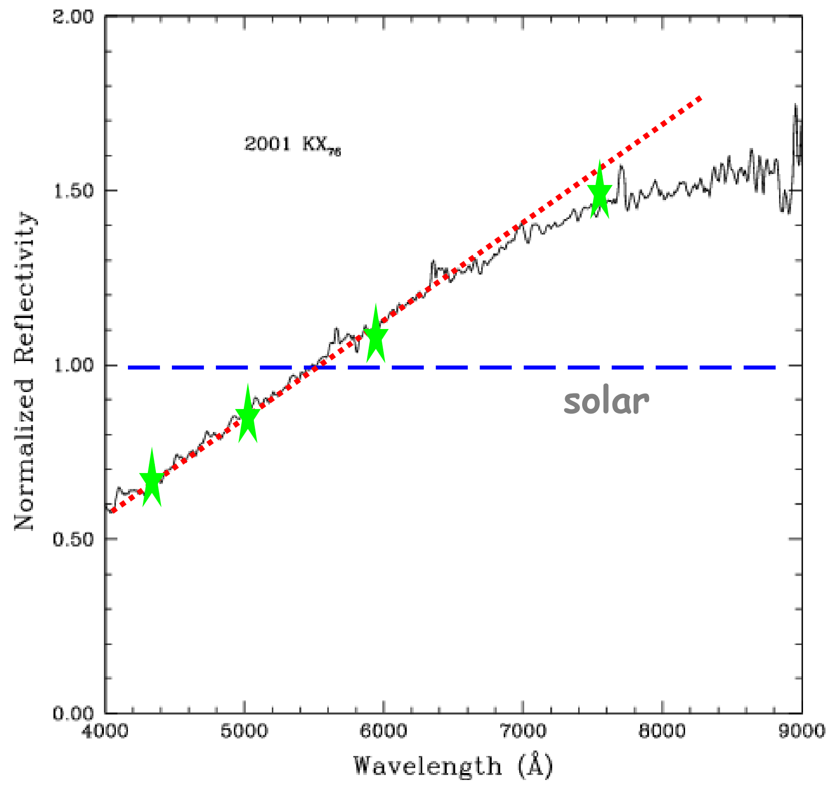

Composition/Taxonomy

- Classification scheme based on telescopic (reflectance spectroscopy and/or photometry) and (few) flyby observations, no in-situ/lab analysis available (Hayabusa still to come)
- Main taxonomic classes (more classes exist, see table):
  - Indications/examples for differentiation of the internal structure of asteroids exists, however also for non-differentiation

    Note: similarities between asteroid and meteorite spectra are used for classification and identification of surface materials
  - A, S, V, R types: pyroxene and olivine absorptions

    ➔ silicate/basaltic bodies, heated material from early period of the Sun

    could come from mantle of a differentiated body
  - E, M, T types: metal-rich absorptions

    ➔ from inner metal core or mantle of differentiated body (wet – hydrated, dry - anhydrous)
  - C, D, G, P types: carbon+organics, low albedo objects, mostly featureless

    ➔ primitive material in two forms:

    (wet – dry)
- Meteorite link:
  - Orbit similarity

    meteorites originate – in parts – from asteroids
  - Spectrum similarity

    → indirect evidences, but with very useful conclusions

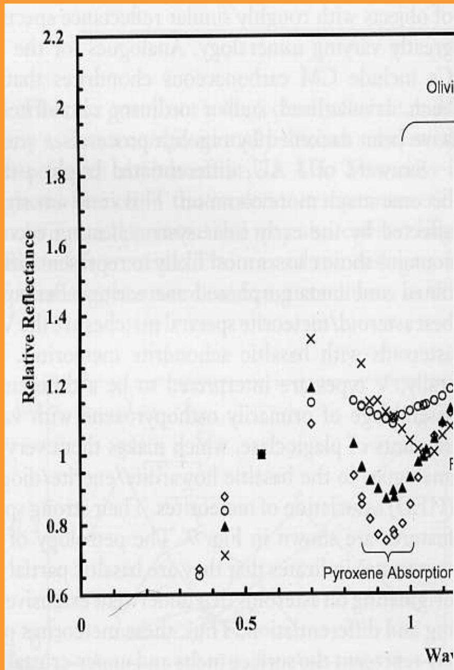

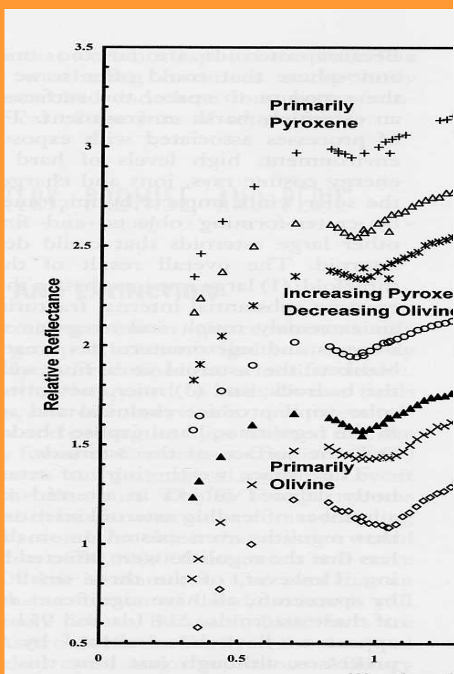

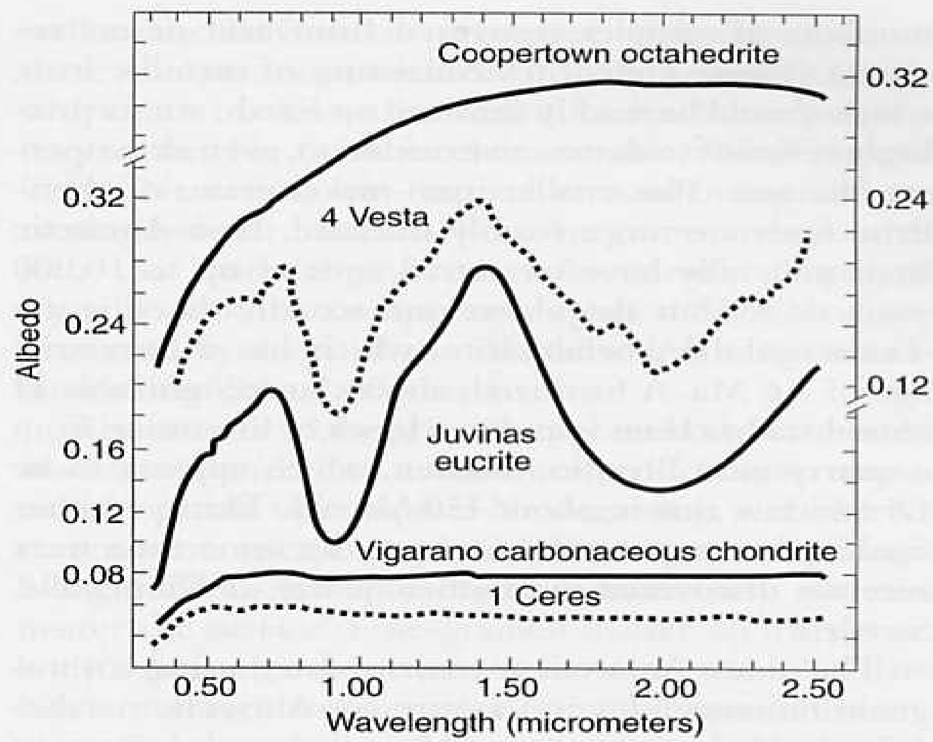

FIGURE 16 Spectral reflectances of the Coopertown IIIE coarse octahedrite, Juvinas eucrite and V-class asteroid 4 Vesta, and Vigarano C3V chondrite and G-class asteroid 1 Ceres. The albedo scale for all but Coopertown is on the left; that for Coopertown is on the right. Solid lines delineate meteorite spectra and dashed lines define asteroid spectra. (Courtesy of Dr. Lucy-Ann McFadden, University of Maryland.)

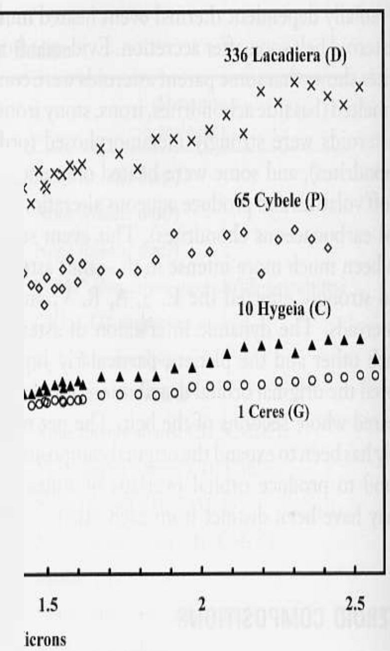

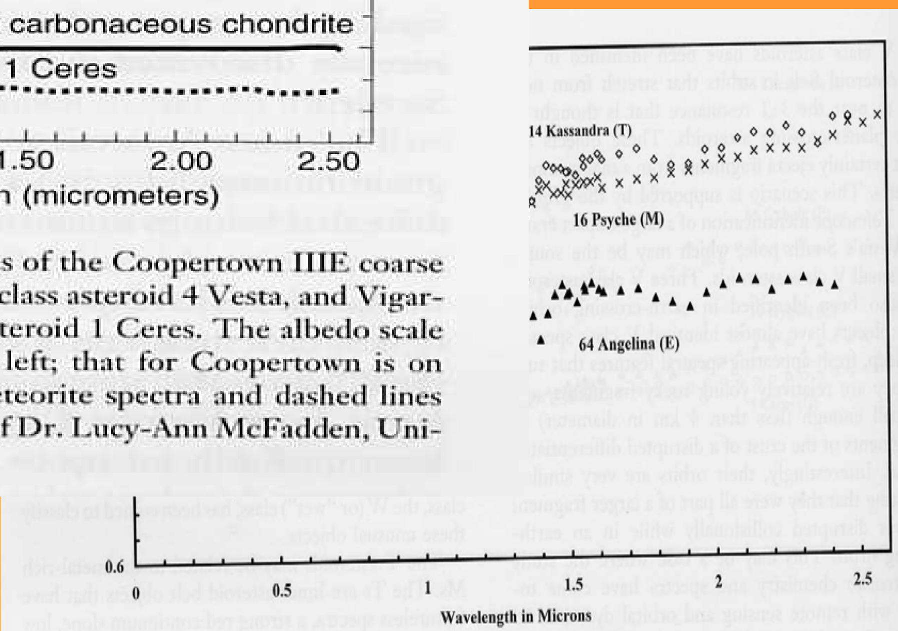

FIGURE 10 Red-sloped M, T, and E classes. These asteroids lack strong absorptions, but have large differences in albedo.

- **<u>Taxonomic class distribution in belt:</u>**
  - Non-uniform
    - Primitive classes in the outer part of the belt
    - Silicate – metal-rich classes in center and inner belt
  - Scenario: differentiation of object interior possible in inner belt due to heating by the early Sun (T-Tauri phase), some larger asteroids in central zone of the belt may have developed molten interiors due to gravitational/radioactive heating

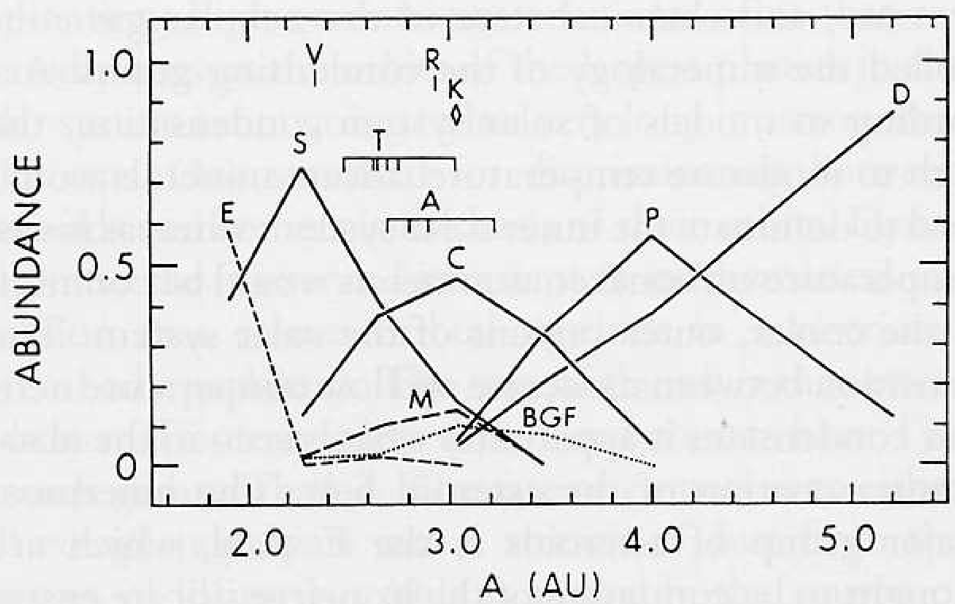

FIGURE 7 Distribution of taxonomic classes from Bell *et a.* (1989). (Courtesy of University of Arizona Press.)

Radar image of 2000 PH5

Sizes, Shapes, Rotation

- Sizes:
  - 1000km → m → mm etc.
  - Only a few ones > 500km diameter
  - Size distribution N versus mass m: $N(m) \sim m^{-3}$

    ➔ indicative for collision dominated size distribution
- Shapes:
  - Irregular except largest ones (spacecraft + radar + lightcurves)
  - Triaxial eelipsoids
- Rotation:
  - Fast rotators more frequent (irregular periodic lightcurves)

    ➔ in agreement with collision scenario, but strong bias from observations (long periods need longer observing time)

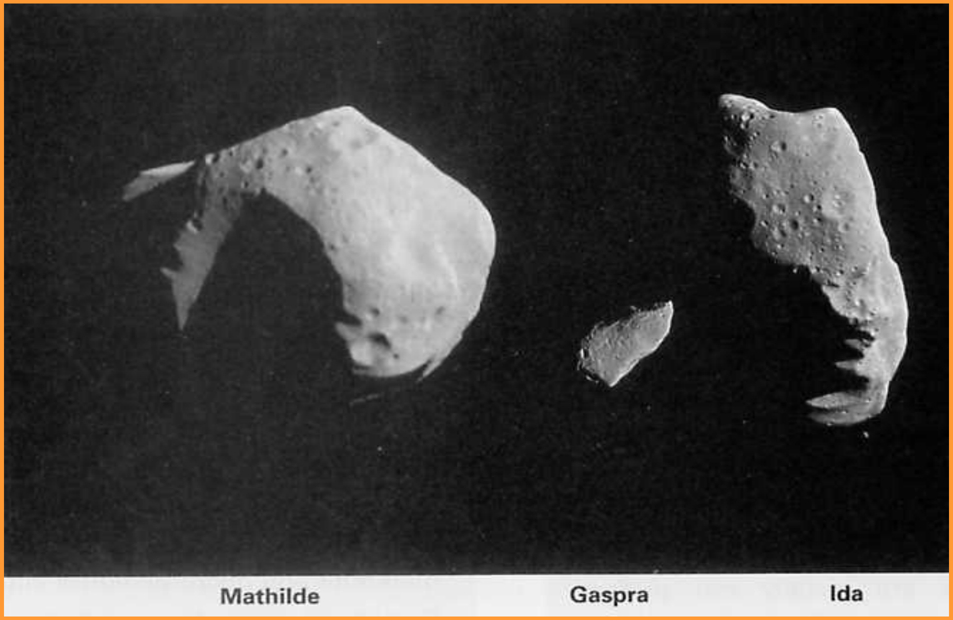

Eros by Shoemaker

1999 SF56 by Hayabusa

Meteorites

- **Summary**
  - Differentiated (associated with asteroids) and undifferentiated (primitive) meteorites
  - Chondrites: ‚uniform‘ age 4.6 10^9 y = age of the solar system
  - Solar composition (except volatile elements)
  - Organics found (L aminoacids)
  - Some isotopic peculiarities indicate non-uniform mixture of solar nebula

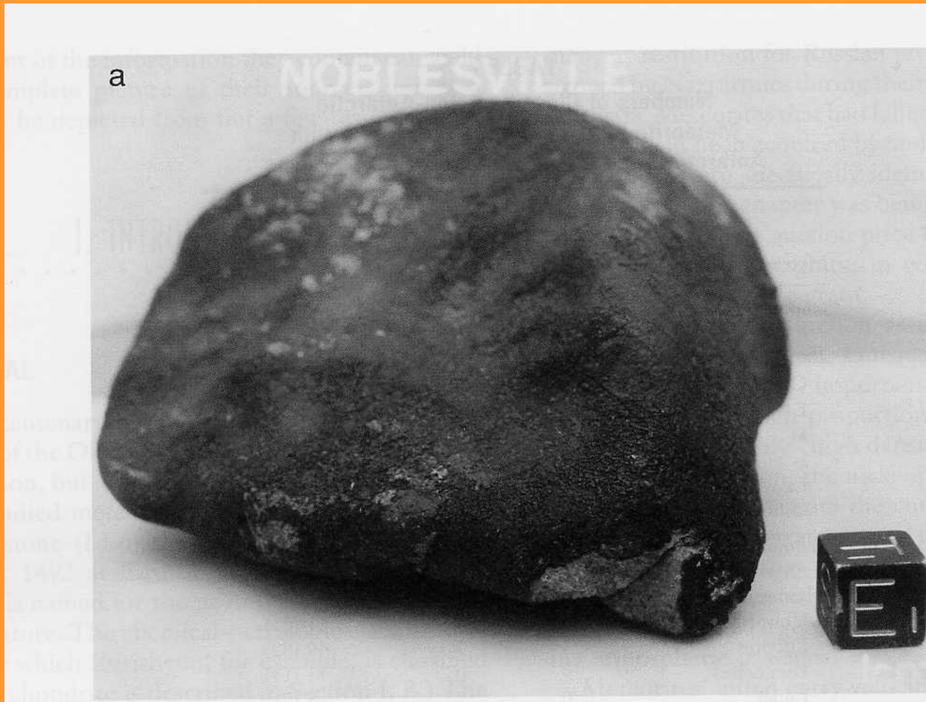

Meteorite with crust

Only the upper few cms are heated during entry in the atmosphere, the interior remains at deeply frozen temperature

Mars meteorite (SNC)

With signature of atmospheric ablations

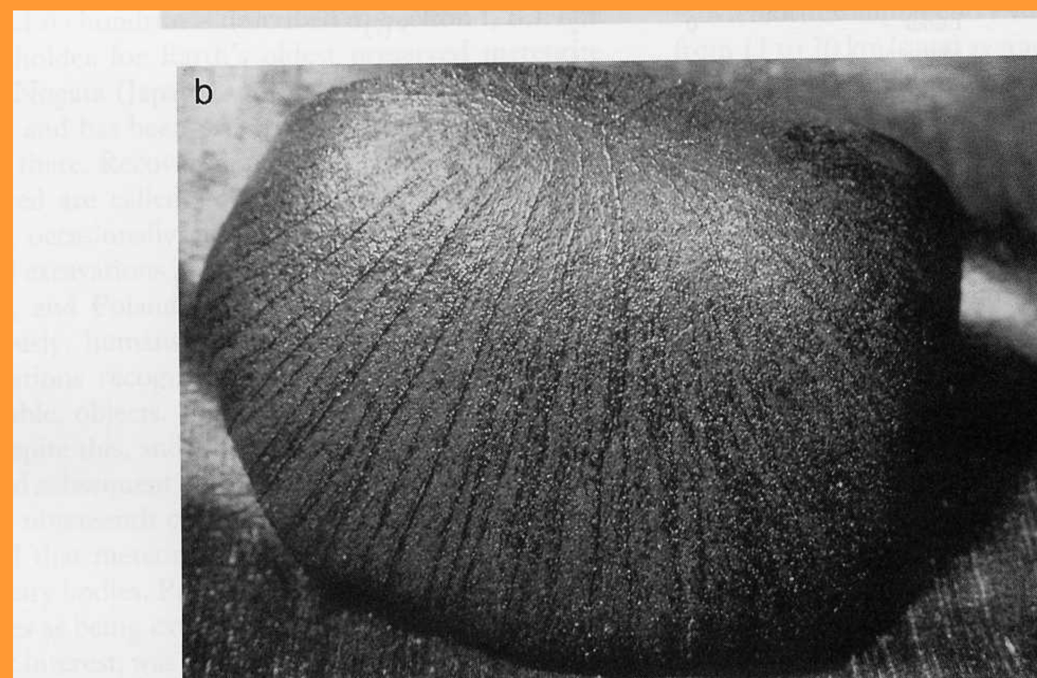

Meteorites in the sky

and hitting a car

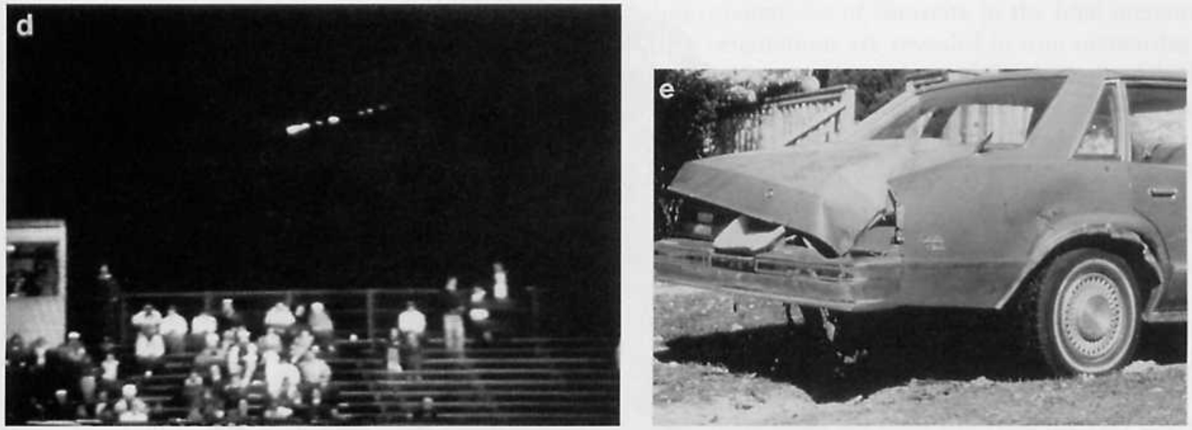

FIGURE 5 *(continued)*

Large meteoroids: Above, a fireball (shown by arrow) of an 80 m object with estimated mass of 1 MTonne, that apparently skipped out of the atmosphere, observed on August 10, 1972 moving left to right over Grand Teton National Park. (Photo courtesy of Dennis Milon) Below, the 1-km diameter Meteor Crater in Arizona formed by the explosive impact of the Canyon Diablo IA octahedrite meteoroid about 50 ka ago. (Photo courtesy of Allan E. Morton)

Allende meteorite

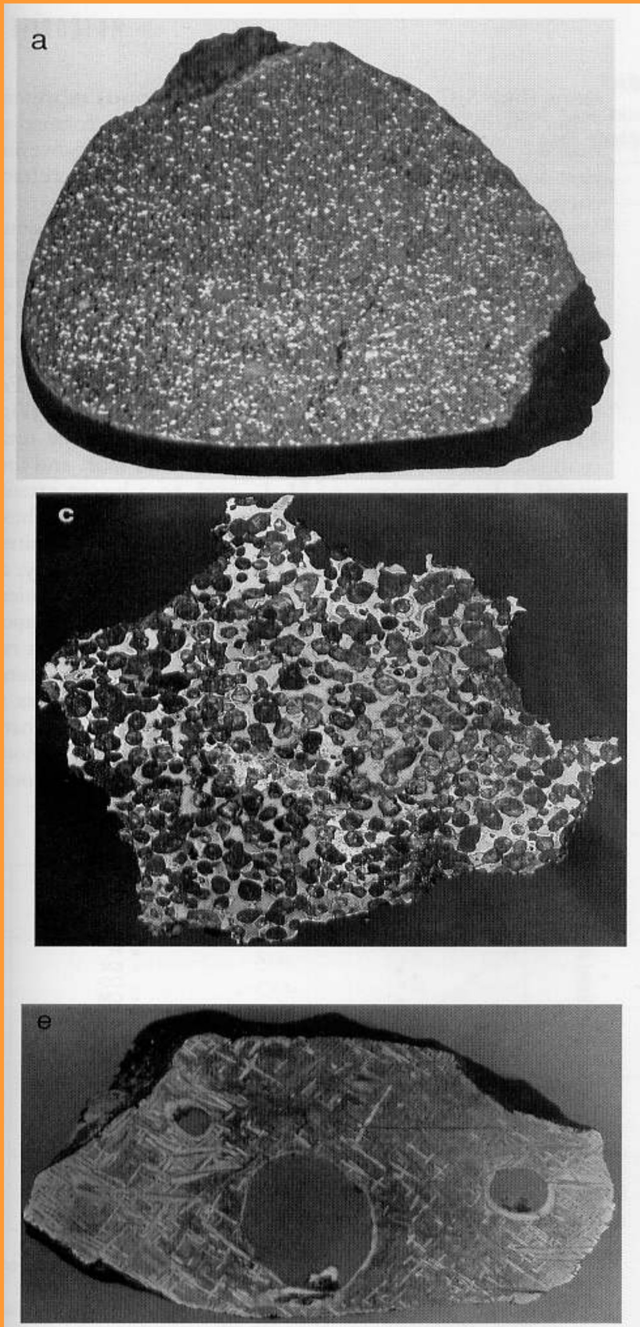

Meteorite - Types

Chondrites (spherical chondrules are present)

undifferentiated

Achondrites

differentiated

Nickel-Iron

differentiated

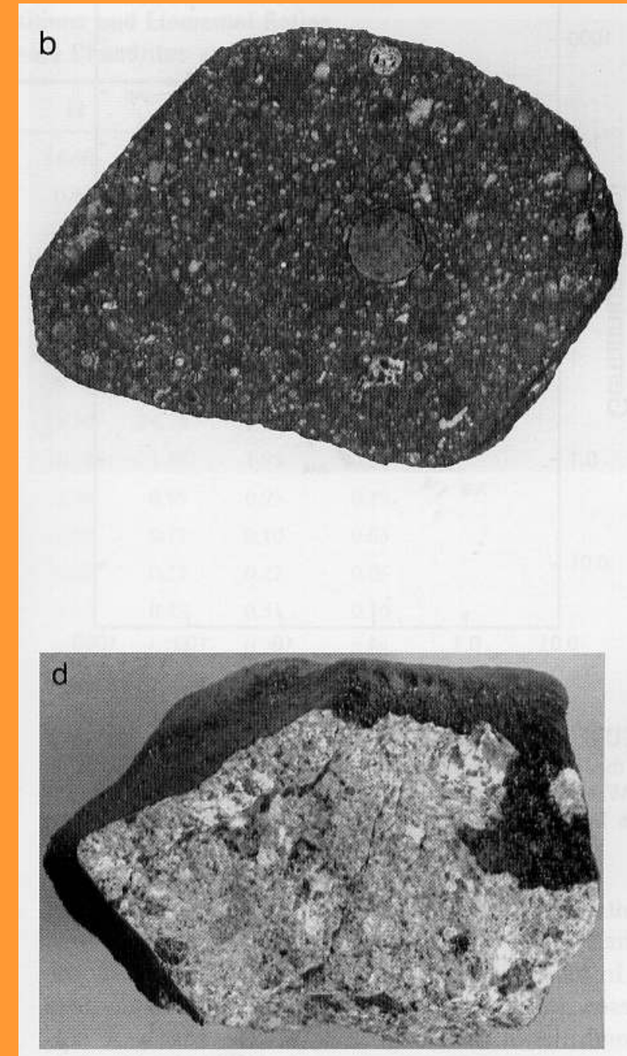

Tectides

terrestrial molten impact ejecta

not considered

Classification

- **Differentiated meteorites:** contain processed material, i.e. were part of a larger differentiated body and became meteorite as a collision product

  Iron (4 %), Stony-Iron (1%), Achondrites (9%)

  molten core, mantle-crust, crust of asteroids

  ➔ differentiated meteorites have a clear link to asteroids

  – Widmanstätten pattern in iron meteorites: Ni content determines crystalisation

  → zones have different Ni content and crystallised at different times

- **Undifferentiated meteorites:** most original, unprocessed material from Solar System formation or before, chondrite types classified by iron content

  normal Chondrites (81 %), carbonaceous Chondrites (5 %)

  chondrule: spherical inclusion of silicate (olivine etc.) in surrounding matrix, created by melting and rapid cooling (re-crystallisation at ~1600K) process at zero gravity

  ➔ either during early phase of the Sun or existent already before formation of the solar system (interstellar grains)

  matrix material is produced by gentle aggregation of molecules at surface in space (surface reactions in cold environment under high energy radiation

  → formation of complex - also organic - molecules)

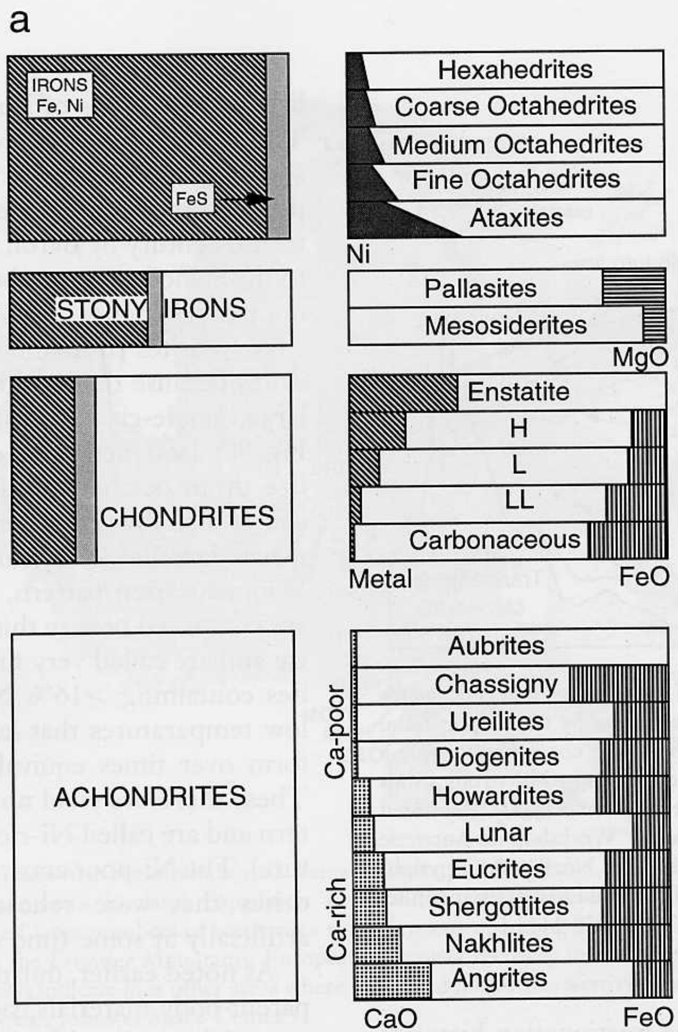

TABLE III

Average Chemical Compositions and Elemental Ratios of Carbonaceous and Ordinary Chondrites and Eucrites

Species[a]	C1	C2M	C3V	H	L	LL	EUC
SiO_2	22.69	28.97	34.00	36.60	39.72	40.60	48.56
TiO_2	0.07	0.13	0.16	0.12	0.12	0.13	0.74
Al_2O_3	1.70	2.17	3.22	2.14	2.25	2.24	12.45
Cr_2O_3	0.32	0.43	0.50	0.52	0.53	0.54	0.36
Fe_2O_3	13.55						
FeO	4.63	22.14	26.83	10.30	14.46	17.39	19.07
MnO	0.21	0.25	0.19	0.31	0.34	0.35	0.45
MgO	15.87	19.88	24.58	23.26	24.73	25.22	7.12
CaO	1.36	1.89	2.62	1.74	1.85	1.92	10.33
Na_2O	0.76	0.43	0.49	0.86	0.95	0.95	0.29
K_2O	0.06	0.06	0.05	0.09	0.11	0.10	0.03
P_2O_5	0.22	0.24	0.25	0.27	0.22	0.22	0.05
H_2O^+	10.80	8.73	0.15	0.32	0.37	0.51	0.30
H_2O^-	6.10	1.67	0.10	0.12	0.09	0.20	0.08
Fe^0		0.14	0.16	15.98	7.03	2.44	0.13
Ni			0.29	1.74	1.24	1.07	0.01
Co			0.01	0.08	0.06	0.05	0.00
FeS	9.08	5.76	4.05	5.43	5.76	5.79	0.14
C	2.80	1.82	0.43	0.11	0.12	0.22	0.00
S (elem)	0.10						
NiO	1.33	1.71					
CoO	0.08	0.08					
NiS			1.72				
CoS			0.08				
SO_3	5.63	1.59					
CO_2	1.50	0.78					
Total	98.86	99.82	99.84	99.99	99.99	99.92	100.07
ΣFe	18.85	21.64	23.60	27.45	21.93	19.63	15.04
Ca/Al	1.08	1.18	1.10	1.11	1.12	1.16	1.12
Mg/Si	0.90	0.89	0.93	0.82	0.80	0.80	0.19
Al/Si	0.085	0.085	0.107	0.066	0.064	0.062	0.290
Ca/Si	0.092	0.100	0.118	0.073	0.071	0.072	0.325
Ti/Si	0.004	0.006	0.006	0.004	0.004	0.004	0.0019
ΣFe/Si	1.78	1.60	1.48	1.60	1.18	1.03	0.66
ΣFe/Ni	18.12	16.15	16.85	15.84	17.73	18.64	
Fe^0/Ni			9.21	5.67	2.29		
Fe^0/ΣFe			0.58	0.32	0.12		

[a] ΣFe includes all iron in the meteorite whether existing in metal (Fe^0), FeS, iron silicates as Fe^{2+} (FeO), or Fe^{3+} (Fe_2O_3). The symbol H_2O^- indicates loosely bound (adsorbed?) water removable by heating up to 110°C; H_2O^+ indicates chemically bound water that can be lost only above this temperature. (Data courteously provided by Dr. E. Jarosewich, Smithsonian Institution.)

Note: almost all meteorites contain iron

First check: magnetism of probe

Verification: spallation isotope

Composition of chondrites is dominated by SiO_2, Fe_2O_3 and MgO

Oxygen Isotopics & Solar Chemistry

- Oxygen Isotopics
  - Concept: mass-dependent process involving O will create $^{17}O/^{18}O$ content with ratio ½ (mass-fractionation: slow process with minor but measurable effects)
  - Earth, moon, many chondrites and some achondrites on ½ fractionation line
  - Some other chondrites deviate

    ➔ solar system was created from a non-heterogenuous (O) isotopic mixture (most likely of pre-solar origin)

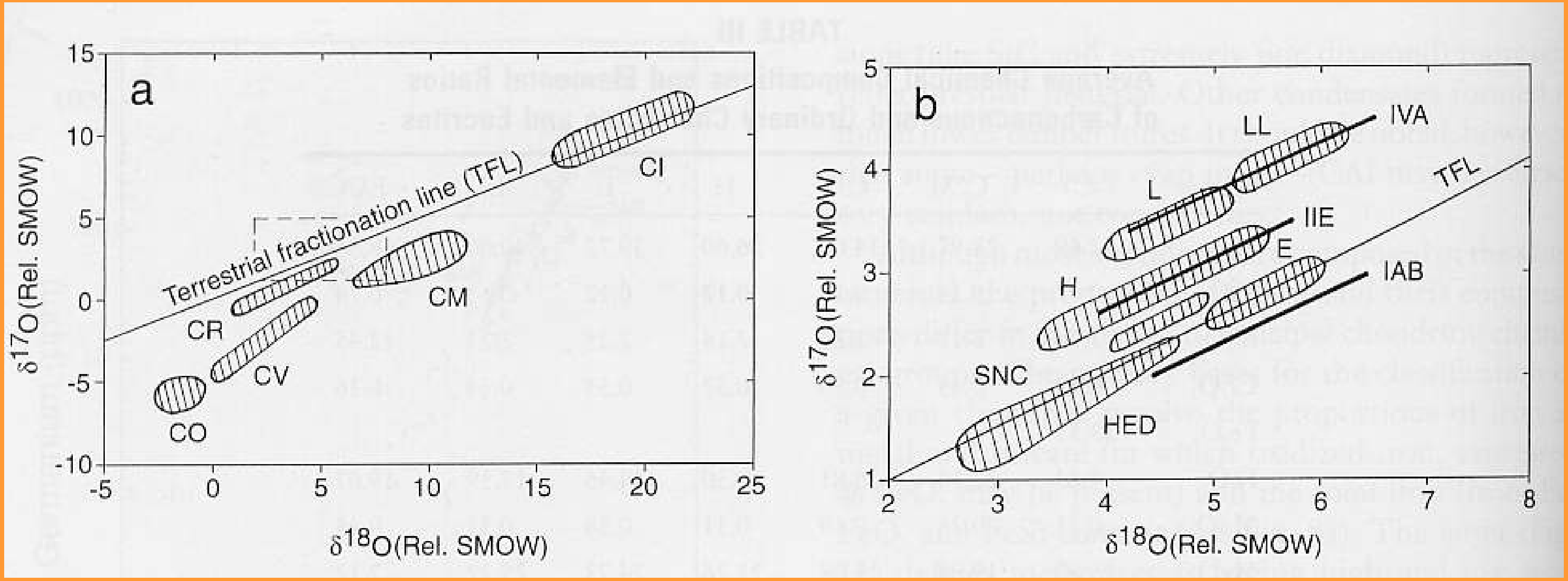

- <u>Isotopic composition CI to solar photosphere:</u>
  - Overall isotopic composition of CI chondrites is basically identical to solar photosphere (with some exceptions: gaseous and light elements, small deviations for mass-fractionation)

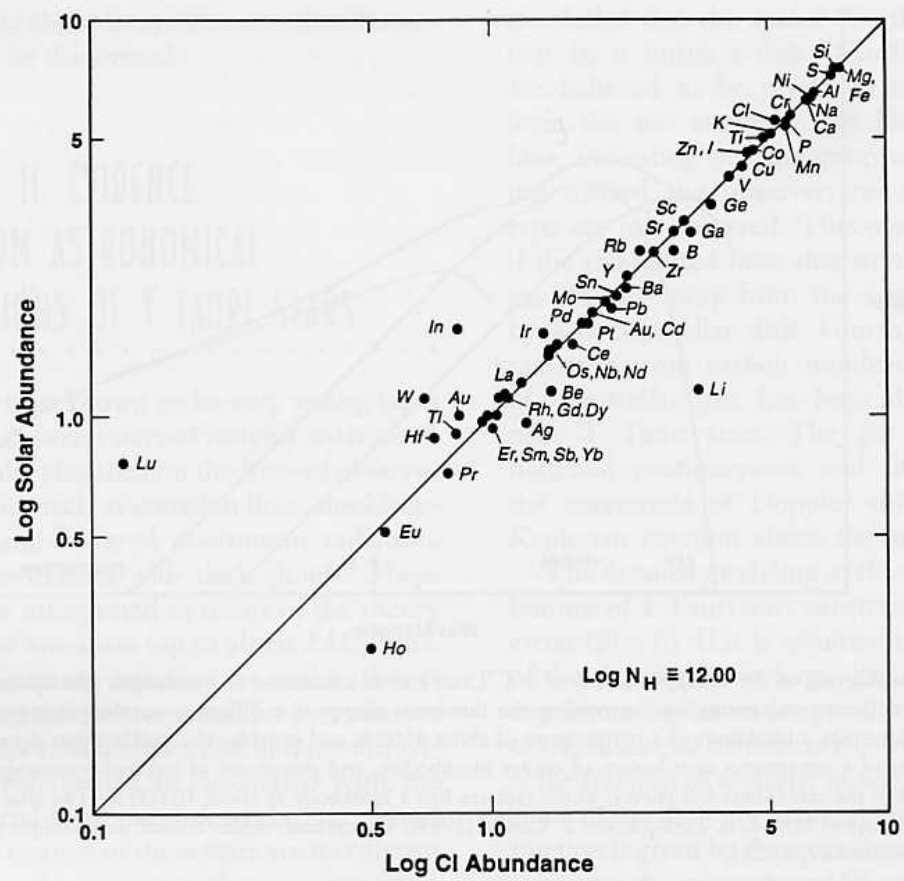

FIGURE 7 Elemental abundances in the solar photosphere are shown on a log–log plot versus those abundances measured in the CI carbonaceous chondrites. The abundances are normalized to 10^{12} hydrogen atoms: log N_H = 12.00. The remarkable 1 : 1 correspondence displayed for all but the most volatile elements is strong evidence for the creation of the CI meteorites out of unfractionated solar material, as well as for the essential homogeneity of the solar nebula. (Even some of the deviations are well understood. For instance, lithium in the Sun is low relative to CI abundances because lithium has been destroyed by nuclear reactions in the Sun.)

Organics & Hydration

- Organics:
  - More than 400 organics compounds identified in meteorites
  - All of non-biogenic, preterrestrial origin, but some with pre-biotic relevance

    (aminoacids of Murchinson & Orgueil L>D chirality)
  - many organics never hotter than 200-300K otherwise it would not exists in carbonaceous chondrites
- Hydration Effects:
  - Many chondrites contain signatures from hydration (chemistry modification due to presence of water – also in liquid form, inclusion of water molecules in mineral lattice)

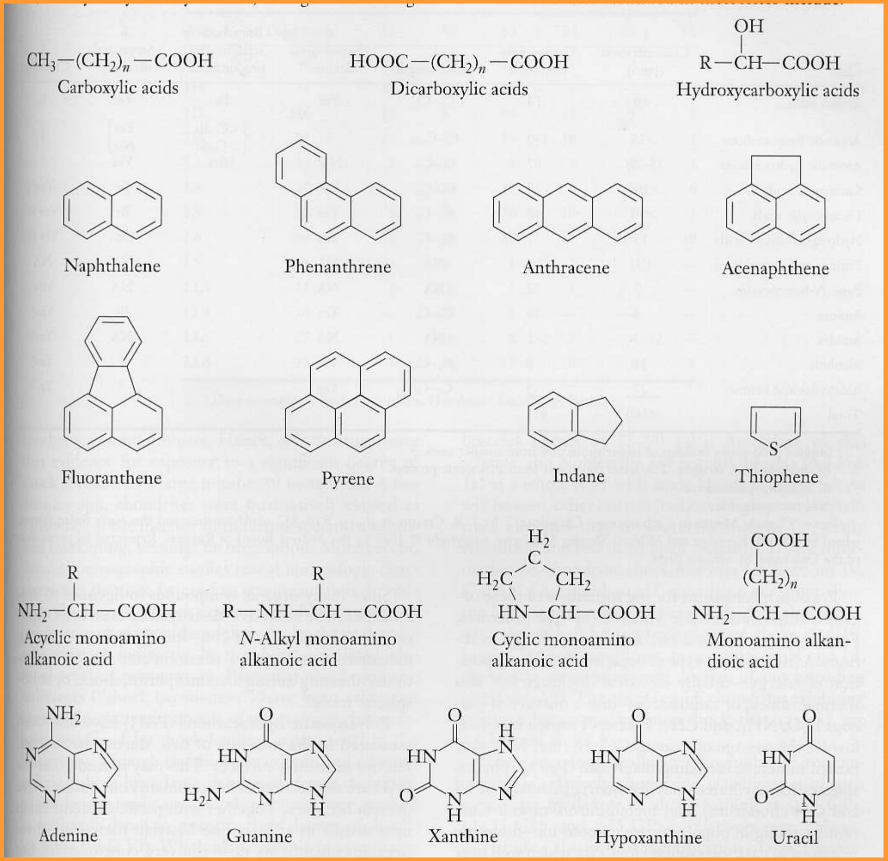

Chronology with Meteorites

- Pre-requisite: state/phase transition locks isotopic ratio in meteorite radioactive and stable nuclides are measurable
  - Number of daughter nuclides D_t at time t

$$D_t = D_o + M_o - M_t = D_o + M_t\,(e^{\lambda t} - 1) \quad (1)$$

D_o, M_o = daughter (unknown), mother (measured) nuclides at ‚locking' time

D_t, M_t = daughter, mother nuclides measured in lab

λ = decay time of isotope

Trick: find/measure stable isotope D_x: $d D_x / dt = 0$

$$(D / D_x)_t = (D / D_x)_o + (M / D_x)_t\,(e^{\lambda t} - 1)$$

Linear relation: $y = I + x * m$ ➔ determine m, i.e. age t of the probe

$$t = 1 / \lambda \; \ln\left(1 + ((D / D_x)_t - (D / D_x)_o) / (M / D_x)_t \right)$$

Formation age = time of crystalisation

Radiation age = duration of high energy irradiation in space

Nuclides used: $^{87}Rb \rightarrow {}^{87}Sr$, $4.9\ 10^{10}$ y

$^{187}Re \rightarrow {}^{187}Os$, $5\ 10^{10}$ y

$^{40}K \rightarrow {}^{40}Ar$, $1.25\ 10^{9}$ y

$^{129}I \rightarrow {}^{129}Xe$, $1.7\ 10^{7}$ y

Solidification age of chondrites

➔ 4.56 10^9 y +/-10^7 y (H-types)

➔ ingredients of solar system agglomerated quasi-simultaneously during a short time

➔ many L-types heated within last 10^9 y (shock-heating)

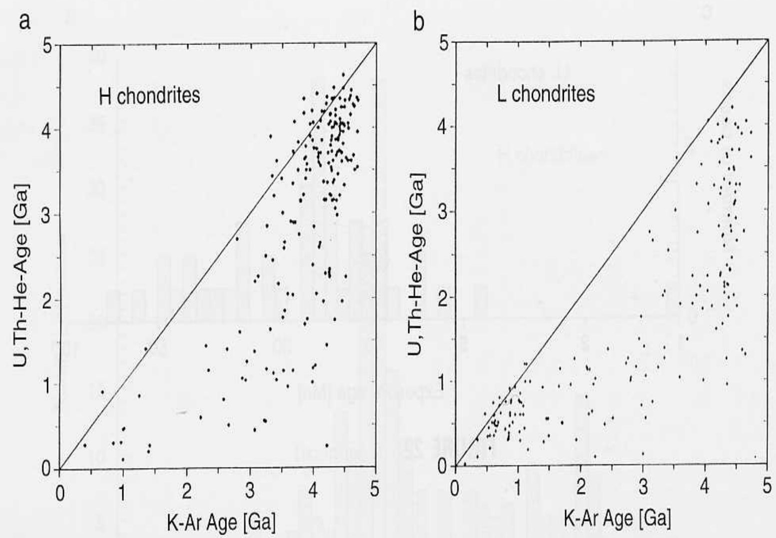

FIGURE 24 Gas retention ages of H and L chondrites. Data obtained from the U, Th–He and K–Ar methods are plotted against each other. The 45° line represents concordant ages. The very different trends indicate that the thermal histories of the two types of ordinary chondrites differ. The concordant long ages of H chondrites suggest that, in general, their parent body or bodies have remained thermally unaltered since they formed 4–4.5 Ga ago. The concordant short ages of L chondrites suggest that they were shock-heated in a major collision(s) 0.1–1.0 Ga ago. Nearly all discordant meteorites lie below the concordance lines because radiogenic ^{4}He is lost far more readily than is radiogenic ^{40}Ar.

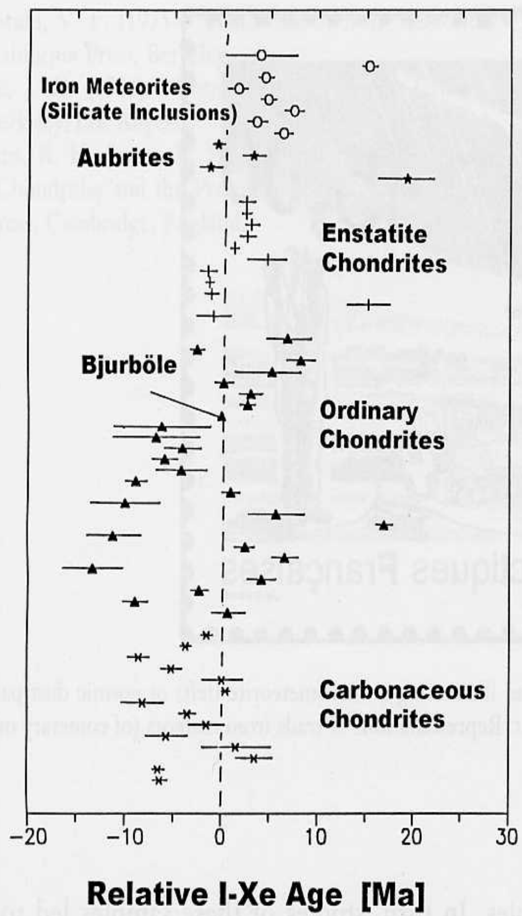

FIGURE 26 ^{129}I–^{129}Xe formation ages for various sorts of chondrites, aubrites, and silicate portions of iron meteorites, relative to that of Bjurböle (older ages to the left and more recent ones to the right).

Comets

- **Summary**
  - Elliptical-hyperbolic orbits
  - Two reservoirs: short period comets & Oort cloud comets
  - Dirty snowball nucleus, km size
  - Main composition: water and silicates, some organics
  - Solar composition, possibly primordial (frozen)

Orbits

- Forms: ellipse+hyperbola
  (parabola easy fit of the other two)
  ➔ no extreme hyperbola found
  (e >> 1; max. 1.005)
  ➔ all observed comets belong to the solar system, hyperbolas caused by non-gravitational forces (reaction forces due to outgassing when active close to the Sun)

- Dynamical classes:
  – Short-period comets (P < 200 y)
  Ecliptic oriented
  captured and dominated by Jupiter gravity (Jupiter family comets)
  ‚old' comets (evolved)
  🡐 originate from Kuiper Belt

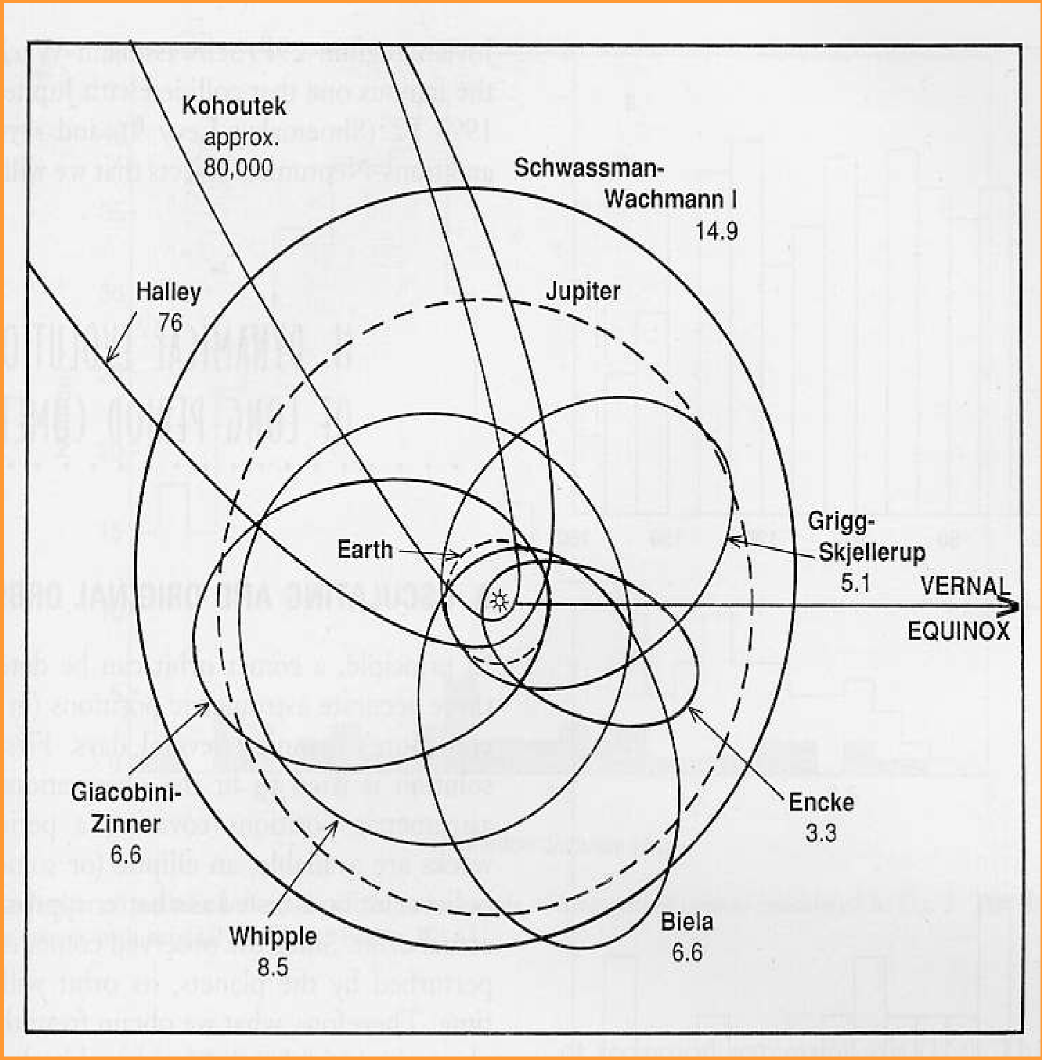

– Long-period comets (P > 200 y)
isotropic distribution, highly eccentric
distribution of inverse semi-major axis peaks for large distances from the Sun
➔ Oort cloud of comets (10^{12}) ***🡐 originate from giant planet region***
less evolved objects (new comets)
perturbations by stars & molecular clouds of our galaxy cause Oort comet to enter into the planetary system

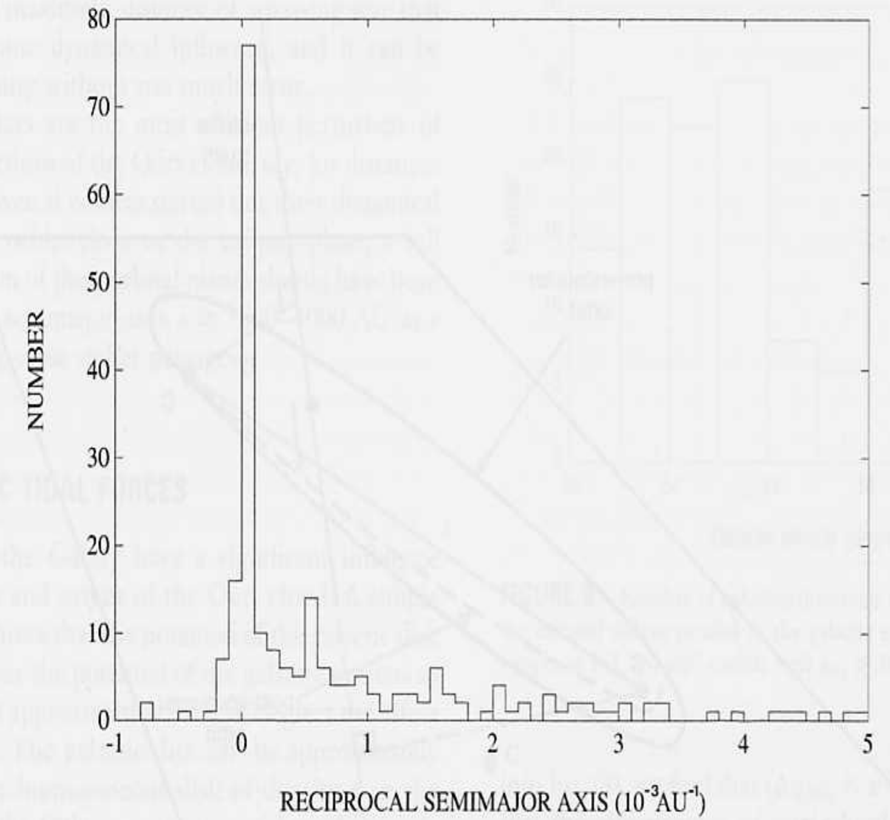

FIGURE 6 Distribution of the original inverse semimajor axes of observed long-period comets with $(1/a)_{orig} < 5 \times 10^{-3}$ AU^{-1}.

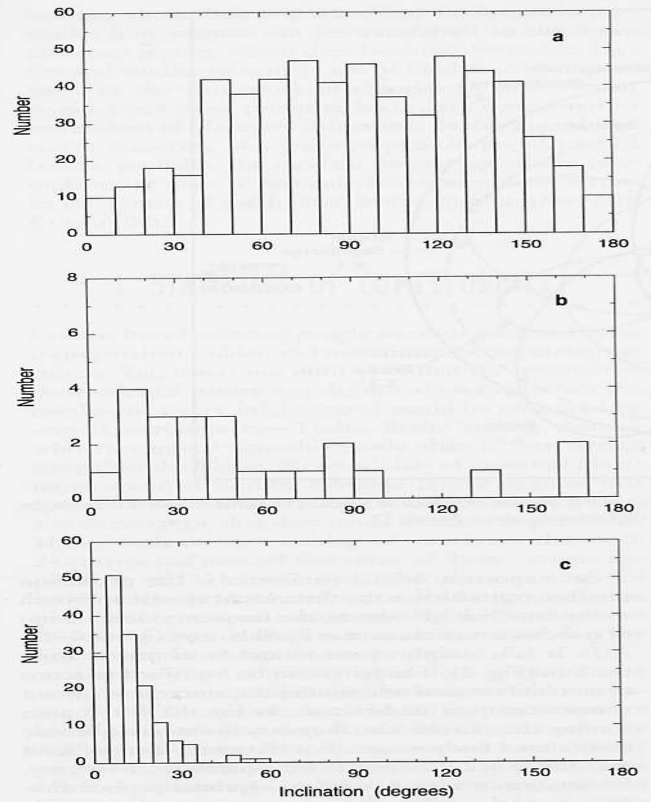

FIGURE 2 Inclination distributions of (a) long-period comets discovered after 1758 (the Kreutz family of sungrazing comets has been considered as a single comet, as well as C/1988F1 and C/1988J1, which move in similar orbits), (b) intermediate-period comets with $20 < P < 200$ yr, and (c) short-period comets with $P \leq 20$ yr.

Nature

- Nucleus: dirty snowball that becomes active when getting close (<5 AU) to the Sun
  - Sizes: a few 100 m – some 10 km
    (Wirtanen 600m) (Hale-Bopp 30km)
  - Shape: irregular with surface structures
  - Albedo: 1-5 %, darkest solar system objects
  - Rotation: a few hours (if measured)
  - Density: 0.1 – 1 g/cm^3 (uncertain) very weak structure (10^4 dyn/cm^2)
  - Different models for nuclei exist
    - Rubble pile (c)
    - Agglomerate with crust (d)

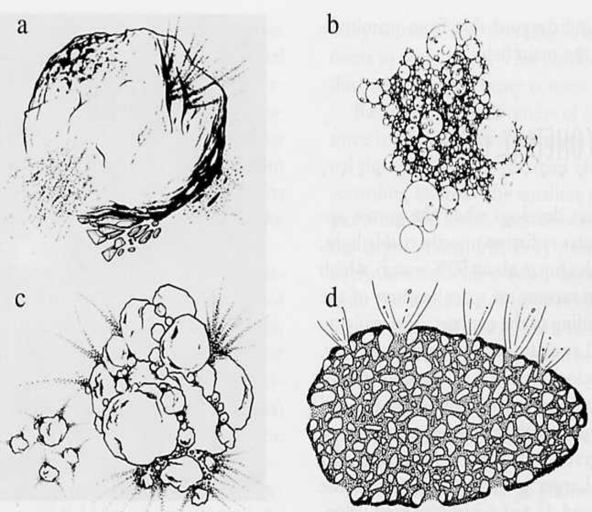

FIGURE 3 Four artist's concepts of suggested models for the structure of cometary nuclei: (a) the icy conglomerate model, (b) the fluffy aggregate model, (c) the primordial rubble pile, and (d) the icy-glue model. Evidence has continued to mount that the fluffy aggregate and the primordial rubble pile are the most likely representations of nucleus structure. All but model (d) were suggested prior to the Halley spacecraft encounters in 1986.

FIGURE 2 A composite image of the nucleus of Comet P/Halley as photographed by the camera onboard the *Giotto* spacecraft on March 14, 1986. The Sun is located toward the left, 29° above the horizontal. Note the elongated and irregular shape of the nucleus, which has dimensions of 16 × 8 × 7 km. The heterogeneity of the irregular surface is well illustrated; several surface features can be seen, including active regions and hills. The smallest features that can be resolved are about 100 m across. (Courtesy of H. U. Keller, Max-Planck-Institut für Aeronomie.)

How do they look like?


Comet Halley by GIOTTO


Comet Borrelly by DEEPSPACE 1

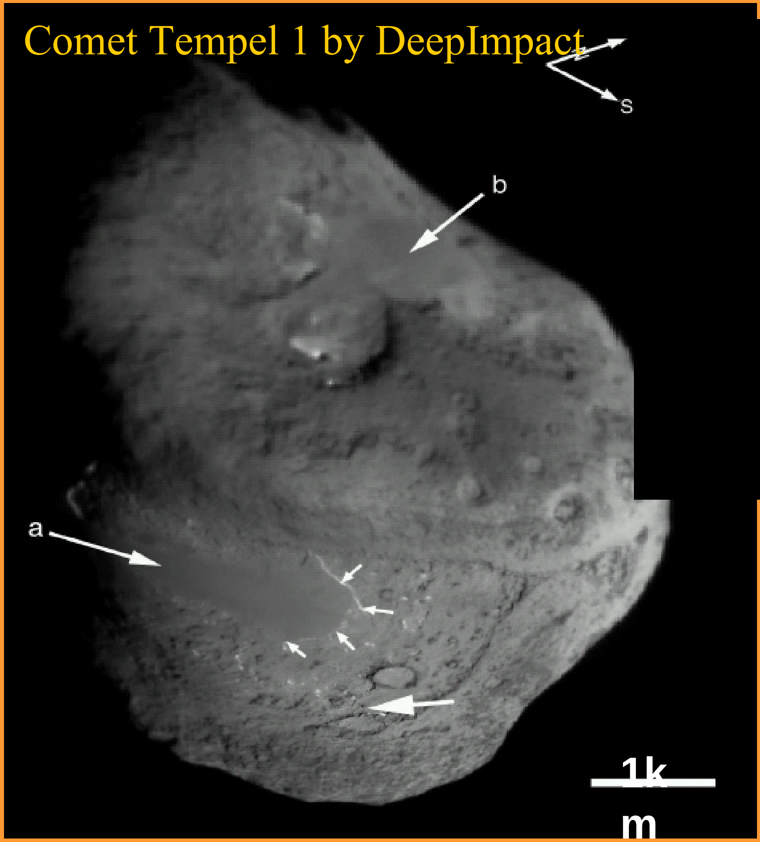

Comet Tempel 1 by DeepImpact

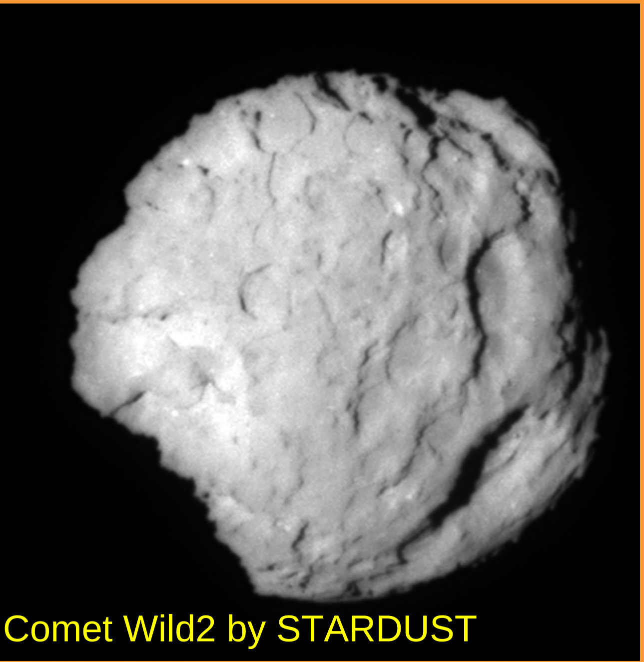
Comet Wild2 by STARDUST

Two movies:

upper: 1P/Halley

lower: 9P/Tempel 1

Coma: activity develops when nucleus is heated close to the Sun (on sunward side)

- Extension: 5 10^4 – 3 10^6 km
- Frozen ice sublimates to gas
    - H_2O: ~80% ice
    - $CO+CO_2+H_2CO$: 4+3+2 (distant activity to several 10 AU)
    - Lots of organics identified
- Embeded dust is accelerated by gas
    - Mass ratio gas:dust 0.1-10
    - Silicate (fosterite), CHON, metallic
    - crystalline (hot) & amorphous (cold) silicates ➔ protosolar nebula got mixed up before comet formation
- Total production rates (gas, dust)
    - 10^{23}-10^{32} molecules/s (several 100 tons/s max)
      ➔ mass loss ~ 10000 revolutions life time in inner solar system
      ➔ continuous supply of comet required
- Crust formation: dust remains or falls back to surface
- Activity frequently localized

- Activity comes from upper few cm-m of the nucleus, nucleus core remains at low temperature 40-80K)

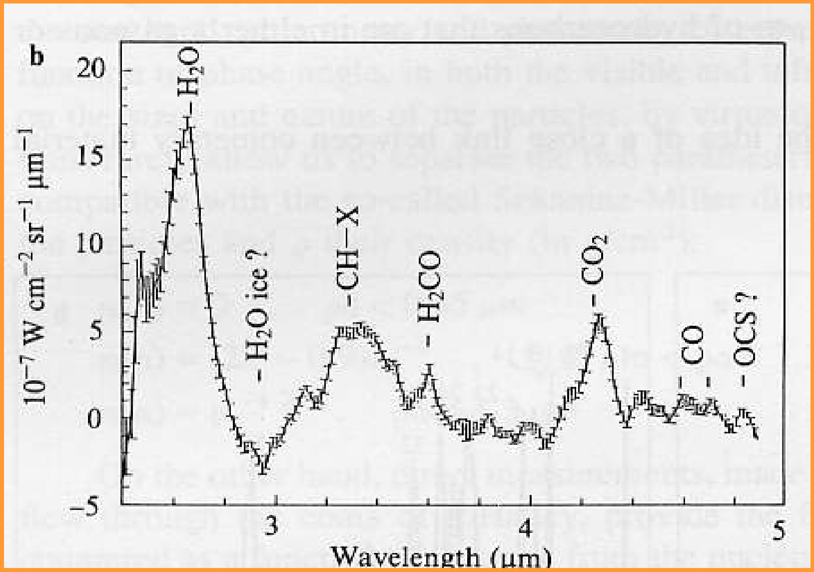

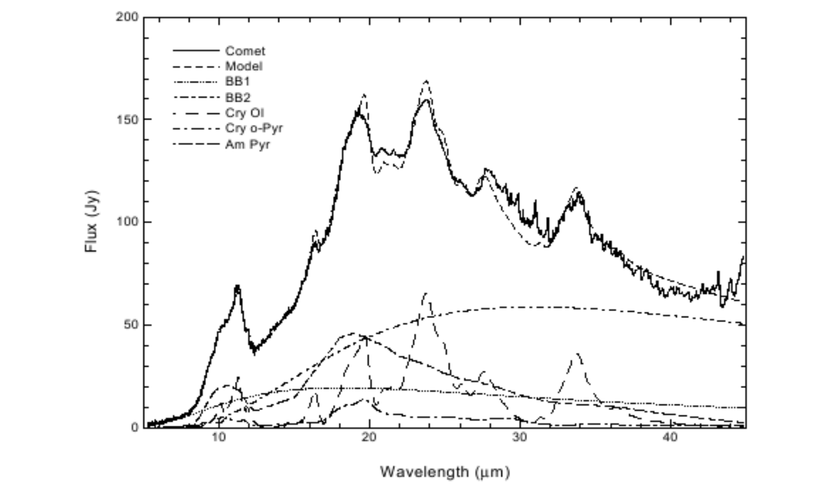

Fig. 2. ISO SWS spectrum of Comet Hale-Bopp at r = 2.8 AU, degraded to $\mathcal{R}$ = 500, compared with a five-component dust model: 280 K blackbody (BB1); 165 K blackbody (BB2); forsterite (Cry Ol 22%); orthopyroxene (Cry o-Pyr 8%); and amorphous pyroxene (Am Pyr 70%). From *Crovisier et al.* (2000).

Dust particle motion

$$\underline{F}_{total} = \underline{F}_{grav} + \underline{F}_{rad} = ma\,\underline{e}_r$$

$$\underline{F}_{grav} = -\gamma mM/r^2\,\underline{e}_r$$

$$\underline{F}_{rad} = LA/4\pi cr^2\ Q\,\underline{e}_r$$

$$\Rightarrow\ \mathbf{ma\,\underline{e}_r = -\gamma mM/r^2\,\underline{e}_r + LA/4\pi cr^2\ Q\,\underline{e}_r}$$

$$\mathbf{= \underline{F}_{grav}\,(1 - ß)}$$

with

$ß = LA/4\pi cQ\gamma mM$
(radiation pressure coefficient)

$\underline{F}_{grav}$ = gravity force
$\underline{F}_{rad}$ = radiation pressure force
a = total aceleration
m = mass of dust particle
M = mass of the Sun
γ = gravity constant
r = distance of the particle from the Sun
L = luminosity of the Sun
A = cross section of the particle
c = velocity of light
Q = radiation pressure efficiency

$\underline{e}_r$ = unit vector in radial direction to the particle

- equation of motion as for gravity
- reduced (even repulsive) effective force in radial direction (Kepler motion)
- recipe for calculating the dust tail geometry
  - calculate comet orbit
  - calculate dust particle orbit
  - calculate difference

➔ synchrones & syndynes

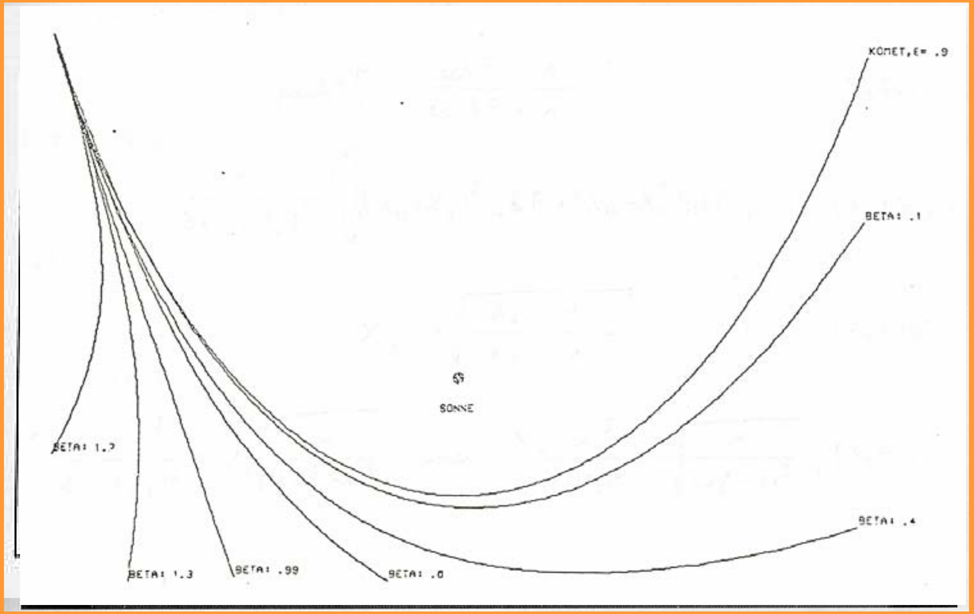

- <u>Ion Tail:</u> ionized gas removed by magnetic field of solar wind

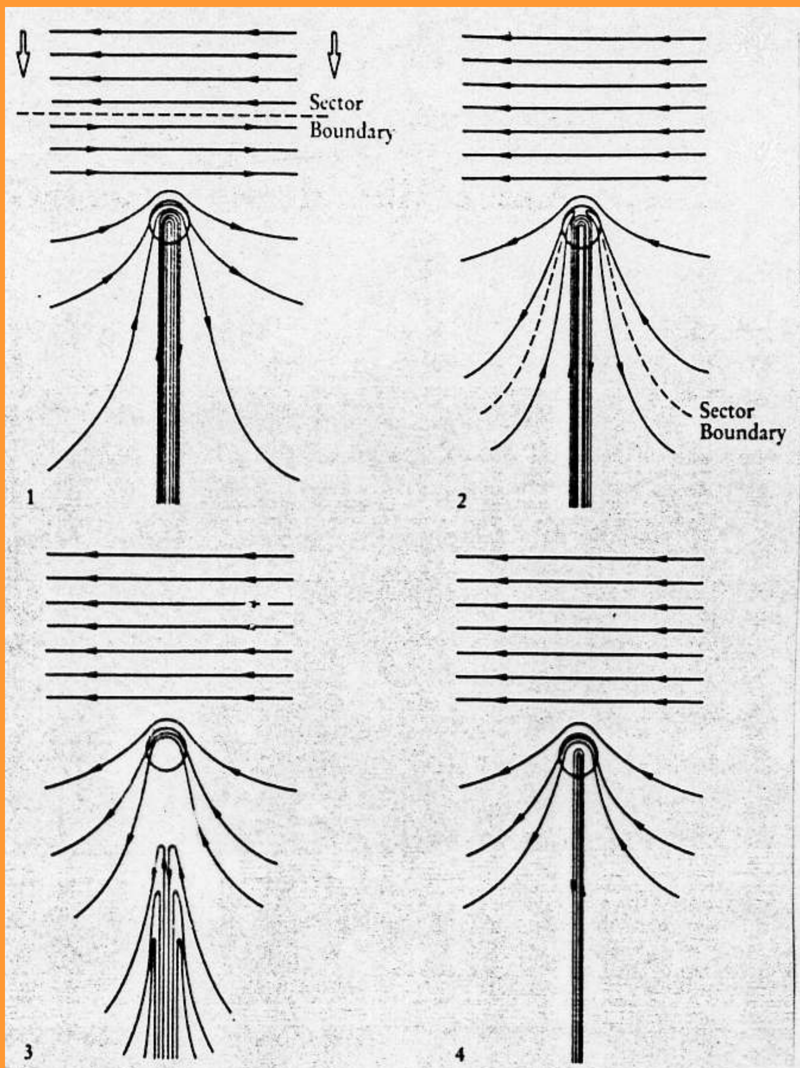

Composition

- Close to solar composition except for volatile elements
- Isotopic composition clearly solar

➔ comets are born in solar system

Table 15.3 Elemental Abundances in Comet Halley, CI-Chondrites, and the Solar Photosphere [a]

Element	Comet P/Halley Dust	Comet P/Halley Dust & Ice	CI-Chondrites	Solar Photosphere
H	2025	4062	520	2.63×10^6
C	814	1010	74	933
N	42	95	5.9	245
O	890	2040	748	1950
Na	10	10	5.61	5.62
Mg	100	100	100	100
Al	6.8	6.8	8.32	7.76
Si	185	185	97.7	93.3
S	72	72	43.7	42.7
K	0.2	0.2	0.363	0.347
Ca	6.3	6.3	6.31	6.03
Ti	0.4	0.4	0.234	0.288
Cr	0.9	0.9	1.32	1.23
Mn	0.5	0.5	0.912	0.646
Fe	52	52	83.2	85.1
Co	0.3	0.3	0.224	0.219
Ni	4.1	4.1	4.90	4.68

[a] atoms/100 Mg

Note: see also Table 3.5 for solar photospheric abundances and Tables 2.1 and 16.9 for abundances on CI-chondrites

Sources: Jessberger, E. K., & Kissel, J., 1991, in *Comets in the post-Halley era* (Newburn, R., Neugebauer, M., & Rahe, J., eds.), Kluwer Acad. Publ., Dortrecht, The Netherlands, Vol. 2, pp. 1075–1092. Mumma, M. J., Weissman, P. R., & Stern, S. A., in *Protostars & planets III* (Levy, E. H., & Lunine, J. I., eds.) Univ. of Arizona Press, Tucson, 1177–1252.

Table 15.4 Relative Abundances in P/Halley (by Number)

Molecule	Abundance	Molecule	Abundance	Molecule	Abundance
H_2O	100	H_2CO	0–5	N_2	~0.02
CH_4	0–2	CH_3OH	~1	NH_3	1–2
CO	7–8	OCS	<7	HCN	≤0.1
CO_2	3	CS_2	1	SO_2	<0.002

Oort Cloud formation – The movie

- **<u>Start:</u>** planetesimals in planetary disk between Jupiter and Neptune
- **<u>Clean-up:</u>** by gravitational scattering of gas gianst
- **<u>Thermalization:</u>** through galactic neighbourhood
- **<u>Return of Oort Cloud comet:</u>** through scattering by galactic neighbourhood

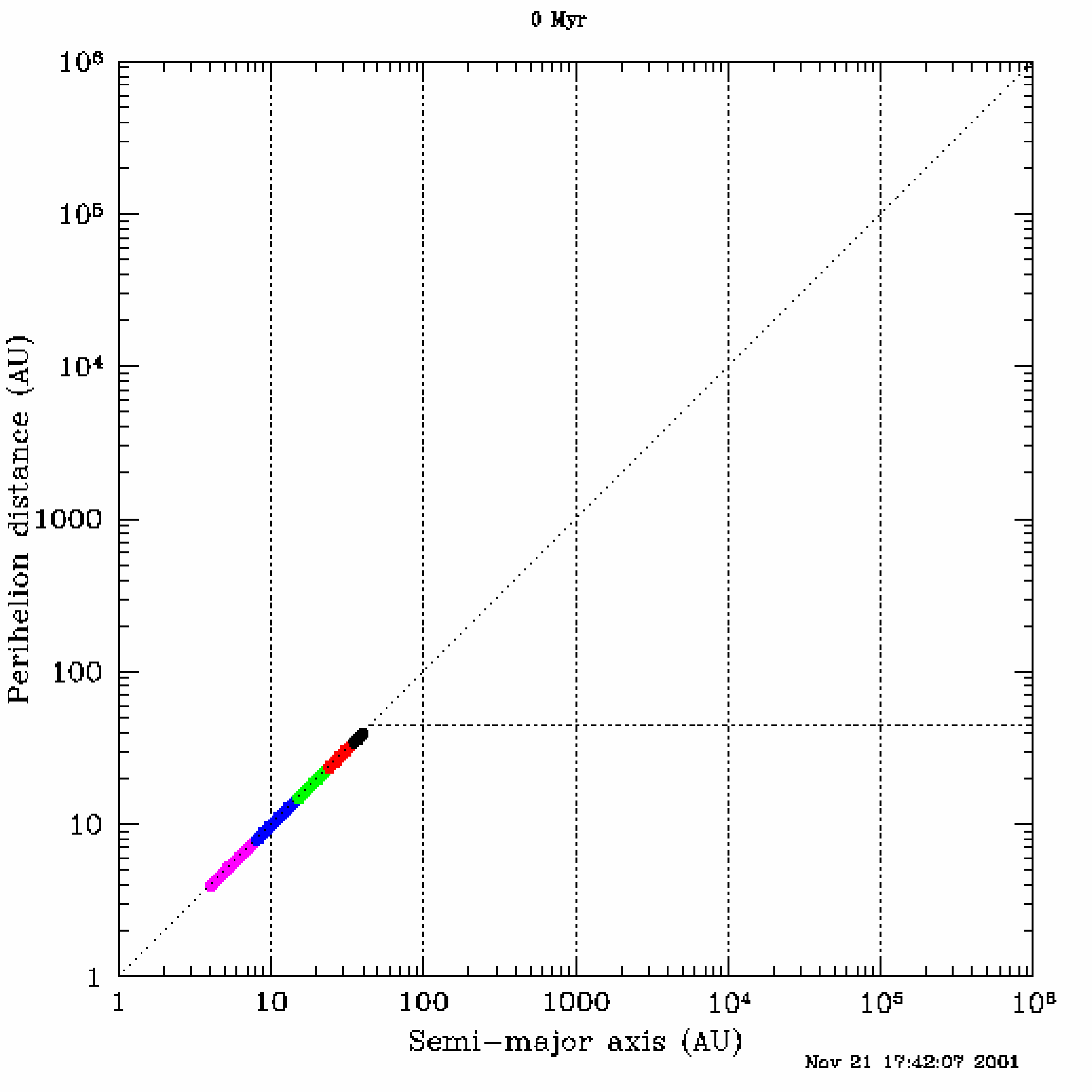

Edgeworth-Kuiper Belt

- **Summary**
  - Orbits mostly between 35-50 AU
  - Large population, with little total mass
  - Collision signatures (double objects, size distribution, collision family)
  - Icy objects (water, methane) with max radius of order 1000km
  - Processed surface: collision, high-energy radiation, activity
  - Reservoir for short-period comets

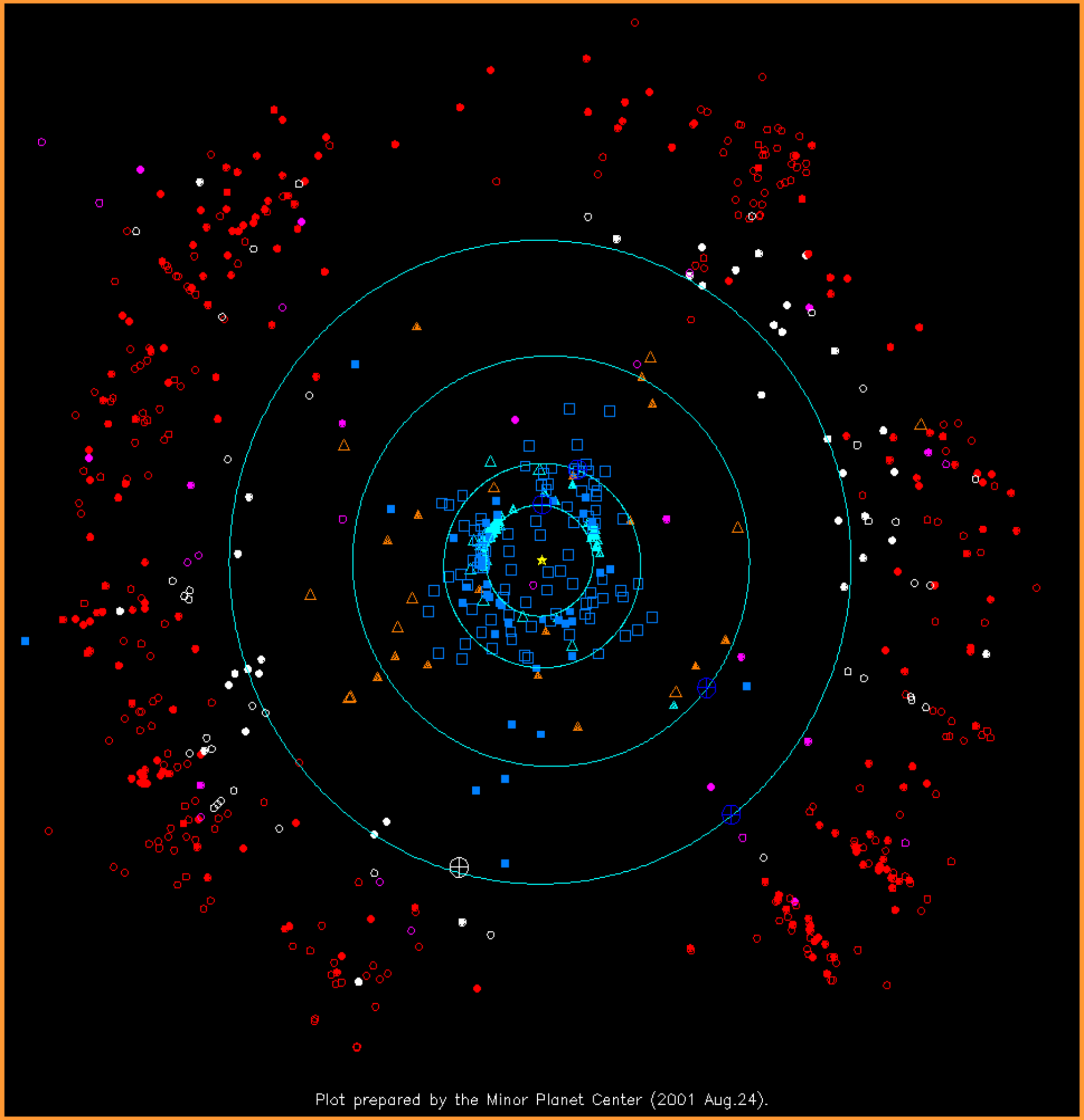

Cubiwanos

Plutinos

ShortP. Comets

Centaurs

Scattered

The Transneptunian Region and ist dynamical Population

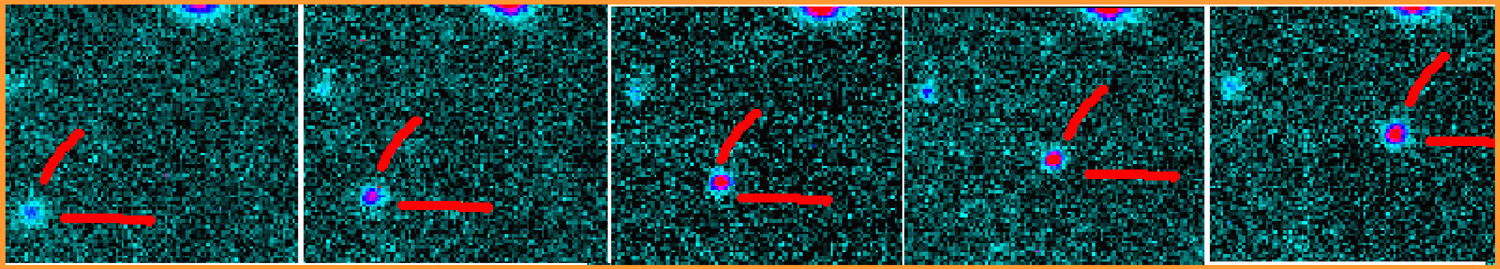

Dynamical Classification

– Plutinos: a ~ 39 AU
e ~ 0.1 - 0.3

➔2:3 resonance with Neptune

– Cubewanos: a ~ 40 - 46 AU
(classical disk) e < 0.1

➔ outside of planet resonance

– Scattered Disk:
a > 50 AU & e > 0.2

– Centaurs:
Jupiter …. Neptune

➔"eccentric" KB members
no resonance beyond 2:1 ~ 50 AU

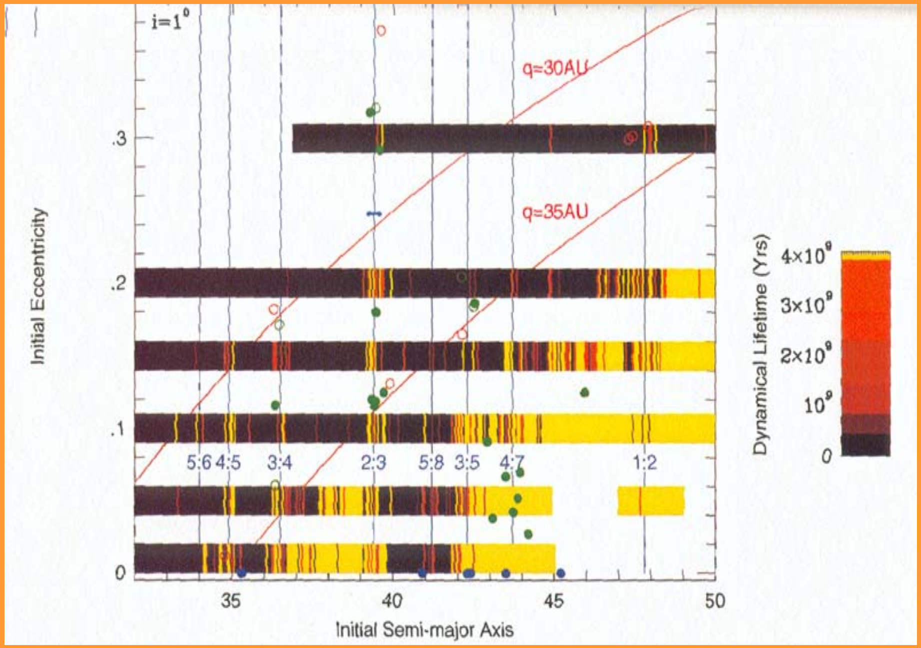

- Plutinos, Cubewanos are in dynamically stable orbits

- Scattered disk will have encounters with planets (Neptune)

- Centaurs are transfered from EKB to inner solar system within ~10 10^6 y

➔ short-period comets

Population Density and Total Mass

- Population density: see table
  - Size distribution = mixture from formation and evolution
  - Slope change for smaller radii
  - ➔ Size distribution gets dominated by collision products
  - more than 10 double TNOs found
  - ➔ produced by large impacts
- Total mass: 0.15 Earth masses (with radius > 100km)

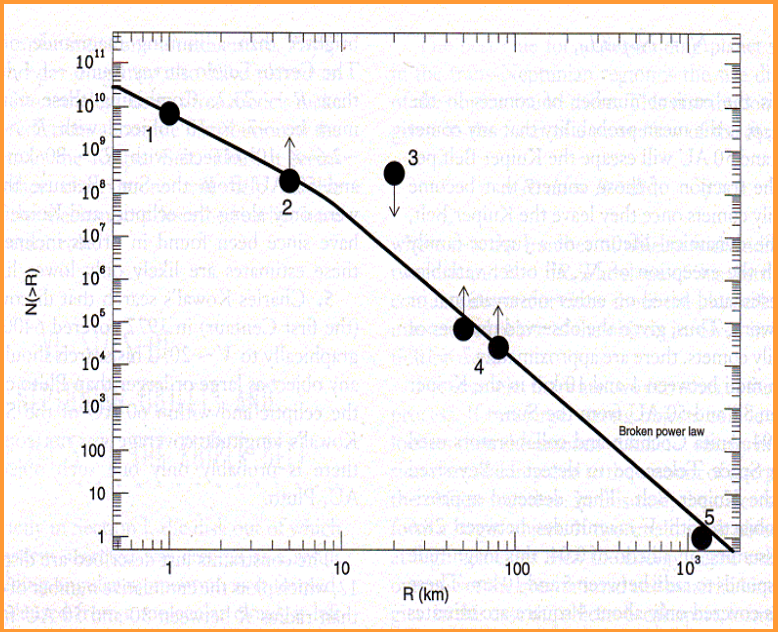

Limit. R Mag. [mag]	Surface Density $[deg^{-2}]$	TNOs In KB < 50 AU	Approx. Radius [km]
< 24	2.7	27000	110
< 26	33	330000	45
< 28	390	3900000	20

Physical Properties

- Size&Shape: 50-1200km radius
  Pluto = largest TNO
  large ones spherical, smaller ones asymmetric
- Albedo: dark (5%) – medium (15%)
  (except when active: >30%)
- Spectrum: some have strong reddening
  ➔ caused by high-energy radiation
  others are neutral compared to Sun
  ➔ due to impact resurfacing or recondensation of temporary atmosphere

Object	Radius [km]	Albedo
Pluto	1150	0.5-0.6
Charon	590	0.3-0.35
1993SC	160	0.02
1996TL66	320	0.03
2000WR106	450	0.07
Chiron	180	0.15
Pholus	190	0.04
Chariklo	300	0.045

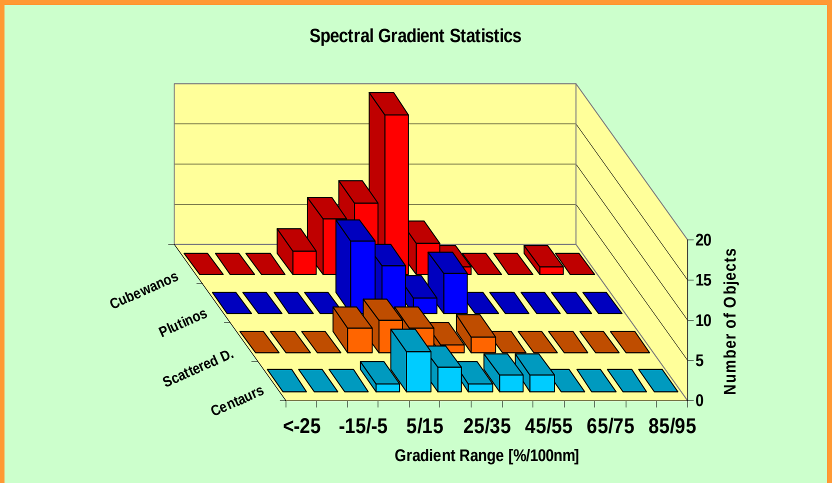

	<-25	-25/-15	-15/-5	-5/+5	5/15	15/25	25/35	35/45	45/55	55/65	65/75	75/85	85/95
Centaurs	0	0	0	1	5	3	1	2	2	0	0	0	0
Scattered D.	0	0	0	3	4	3	1	2	0	0	0	0	0
Plutinos	0	0	0	0	9	6	2	5	0	0	0	0	0
Cubewanos	0	0	0	3	7	9	20	4	1	0	0	1	0

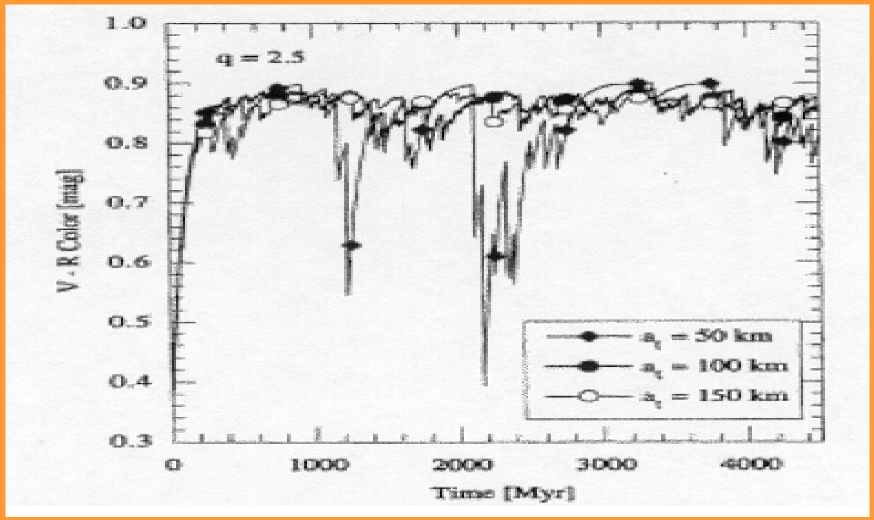

Simulation of reddening changes

- <u>Surface chemistry:</u> some with water/methane ice absorption,
- One case of hydrated silicate dedected → surprise liquid water ?

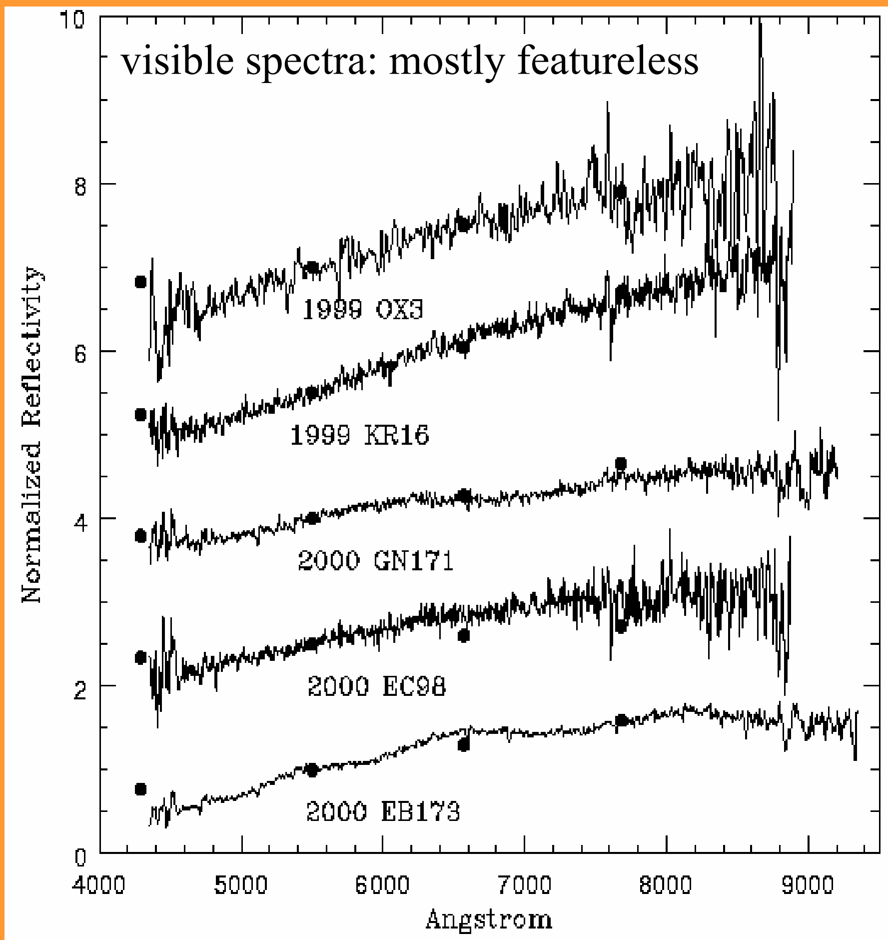

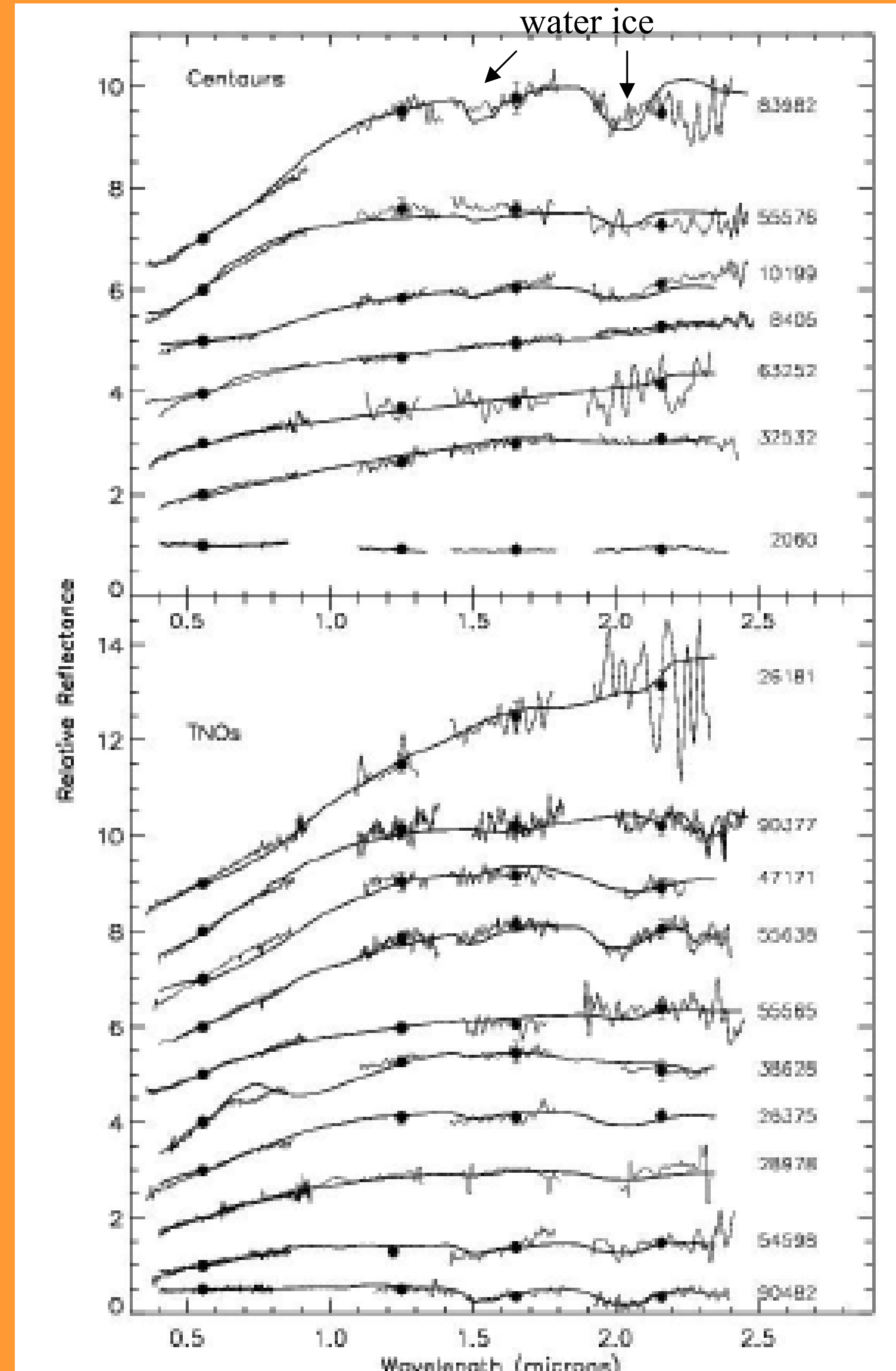

Pluto & Charon (since 1978)

- Orbit: stable in past, chaotic after ~ 2 10^7 y

Size: 1200/600km radius, 2^{nd} largest TNO

- Density: ~1.9 g/cm^3 (high!➔ not only ices)
- Charon synchronous to Pluto orbit (6.4d)
- Albedo: P:0.4-0.6; C:0.3-0.35
- Colours: P = red, C = neutral
- Atmosphere: around perihelion for Pluto
  temporary nature ➔ resurfacing
- Surface: P: CH_4, N_2, CO T ~ 45-60K
  patchy
  C: H_2O, little CH_4 more uniform?

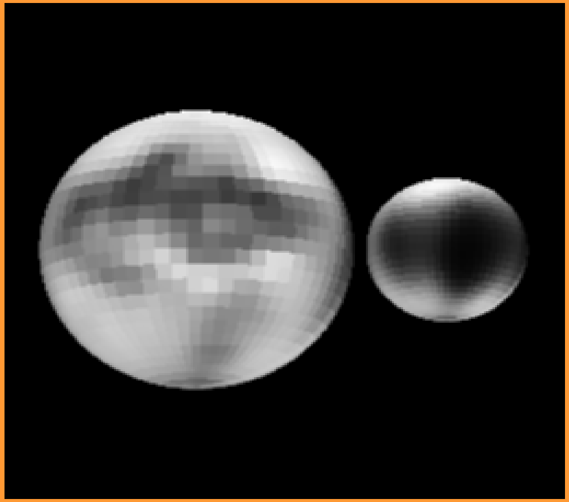

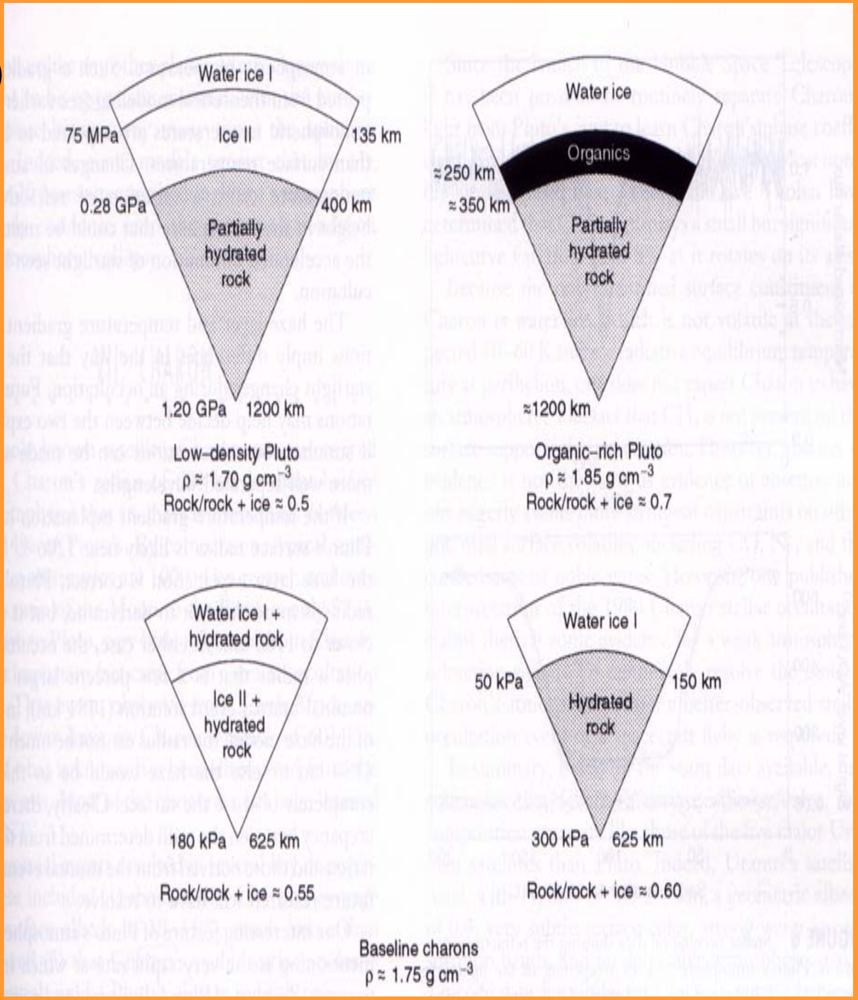

(1) Kuiper Belt formation:
- presence of Pluto puts modelling constraint
Try to make Pluto via accretion from 1m-1km size bodies at 40 AU distance
➔ more 1000-10000 Earth masses needed in Kuiper Belt region
➔ More than one Pluto is formed (Eris & Sedna & Triton)

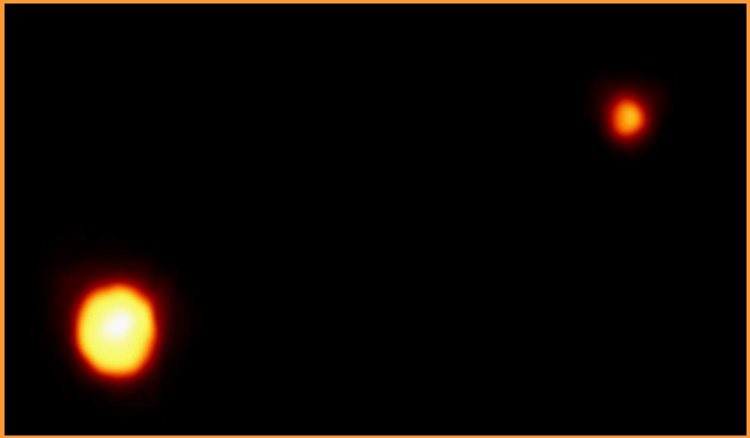

(2) Missing mass problem:
mass surface density of outer planetary system $\sim r^{-2}$ in giant planet region
present Kuiper Belt drop by factor 10^2-10^3

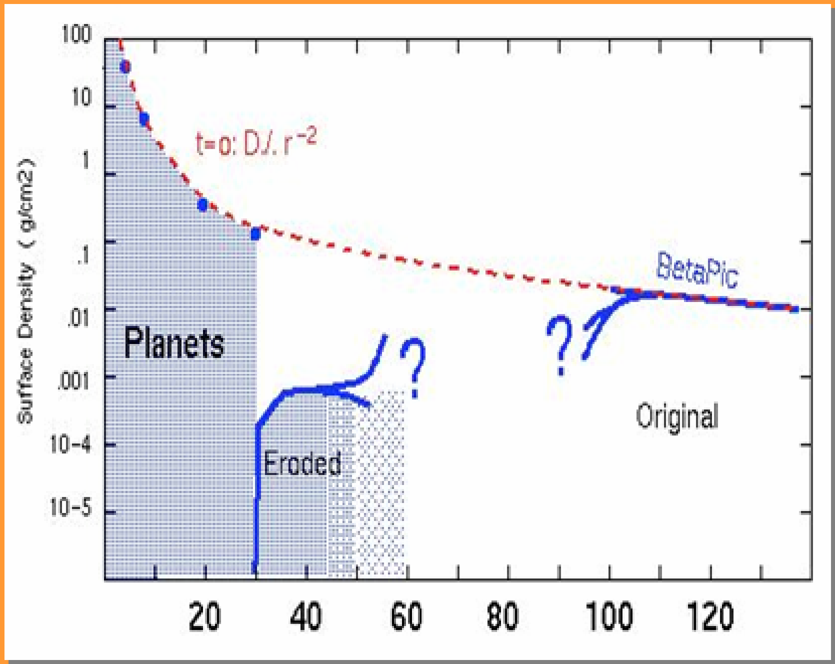

(1)+(2) ➔ originally, the Kuiper Belt may have been massive and may have matched the extension of the mass surface density function

Interplanetary Dust

- **Summary**
  - Interplanetary dust cloud in inner solar system
  - Sources: cometary dust and collision in asteroid belts
  - Short lifetimes ➔ continuous replenishing

Appearance & Detection

- Zodiacal light: visible close to the horizon as diffuse light before/after sunrise/set
  - dust disk around the Sun, ecliptic oriented
  - Sun illuminated micron-size dust
- Meteors: trails of excited mostly atmospheric molecules in entry channel of mm-cm size dust, 120-60km height
- Other detection techniques: see schematics

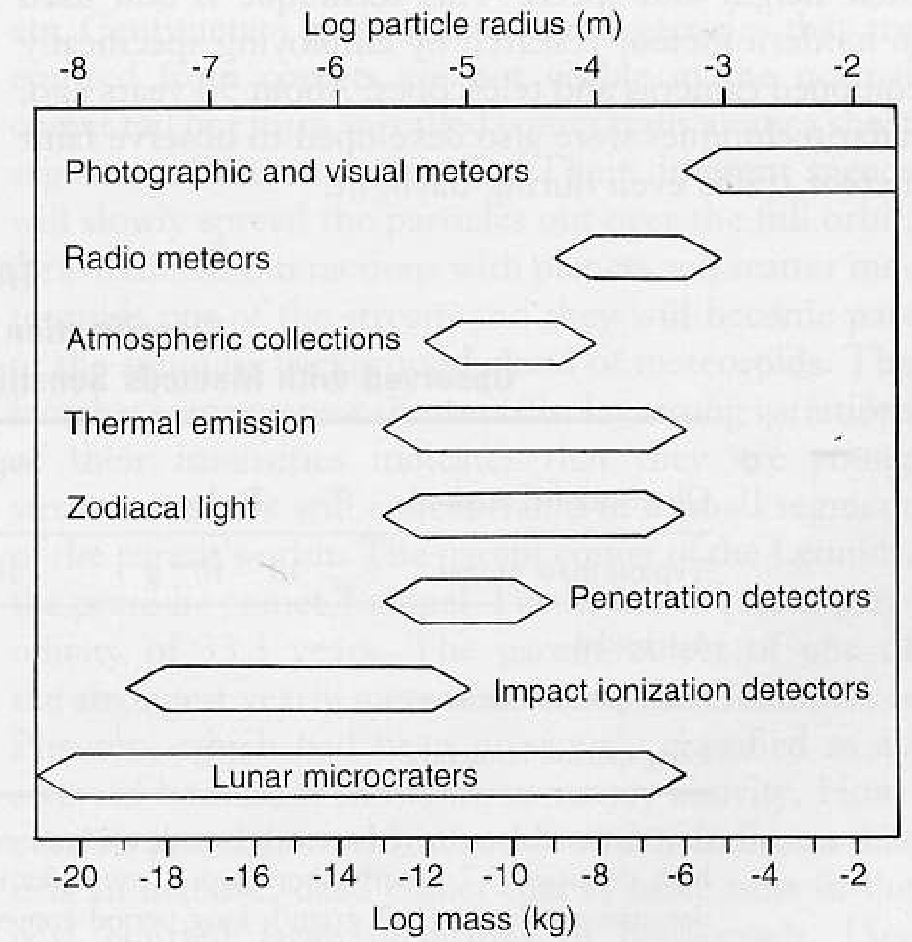

FIGURE 3 Comparison of meteoroid sizes and masses covered by different observational methods.

FIGURE 4 An unusually strong meteor shower (Leonid) was observed on 17 November 1966. The meteor trails seem to radiate from the constellation Leo.

FIGURE 1 Cone of zodiacal light seen in the west one hour after sunset. The ecliptic plane is delineated by Venus at the top of the cone and the crescent moon just above the horizon. (Courtesy of C. Leinert.)

Zodiacal light

Leonid meteor stream

- <u>Meteor streams:</u> enhanced meteor activity with trails converging to the same apparent point in the sky (radiant, meteor streams are named after radiants)
  - Orbits of meteors in stream similar to comets
  - Trails of dust along cometary orbits
    - ➔ Dust particles from comets
    - ➔ Earth passage through trails causes meteor streams

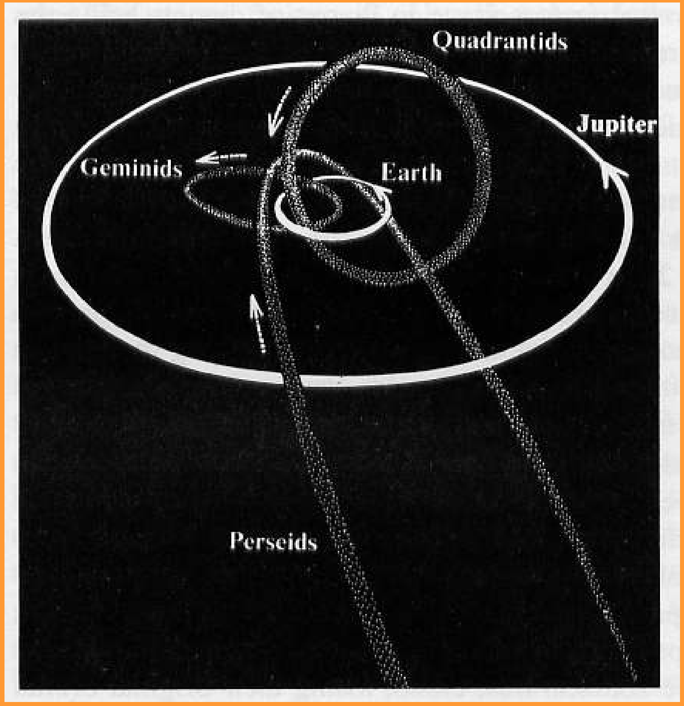

TABLE II

Major Meteor Showers, Date of Shower Maximum, Radiant in Celestial Coordinates (Right Ascension, RA, and Declination, DEC, in Degrees), Geocentric Speed (km/s), Maximum Hourly Rate, and Parent Objects (If Known, Short-Period Comets Are Indicated by P/)[a]

		Radiant				
Name	Date	RA	DEC	Speed	Rate	Parent object
Quadrantids	Jan. 3	230	+49	42	140	
April Lyrids	Apr. 22	271	+34	48	10	Comet 1861 I Thatcher
Eta Aquarids	May 3	336	−2	66	30	P/Halley
June Lyrids	June 16	278	+35	31	10	
S. Delta Aquarids	July 29	333	−17	41	30	
Alpha Capricornids	July 30	307	−10	23	30	P/Honda-Mrkos-Pajdusakova
S. Iota Aquarids	Aug. 5	333	−15	34	15	
N. Delta Aquarids	Aug. 12	339	−5	42	20	
Perseids	Aug. 12	46	+57	59	400 (1993)	P/Swift-Tuttle
N. Iota Aquarids	Aug. 20	327	−6	31	15	
Aurigids	Sept. 1	84	+42	66	30	Comet 1911 II Kiess
Giacobinids	Oct. 9	262	+54	20	10	P/Giacobini-Zinner
Orionids	Oct. 21	95	+16	66	30	P/Halley
Taurids	Nov. 3	51	+14	27	10	P/Encke
Taurids	Nov. 13	58	+22	29	10	P/Encke
Leonids	Nov. 17	152	+22	71	3000 (1966)	P/Tempel-Tuttle
Geminids	Dec. 14	112	+33	34	70	Phaeton
Ursids	Dec. 22	217	+76	33	20	P/Tuttle

[a] After A. F. Cook (1973). *In* "Evolutionary and Physical Properties of Meteoroids" (C. L. Hemenway, P. M. Millman, and A. F. Cook, eds.), pp. 183–192. NASA SP-319, National Aeronautics and Space Administration, Washington, D.C.

Airborne collected interplanetary dust particles (IDPs)

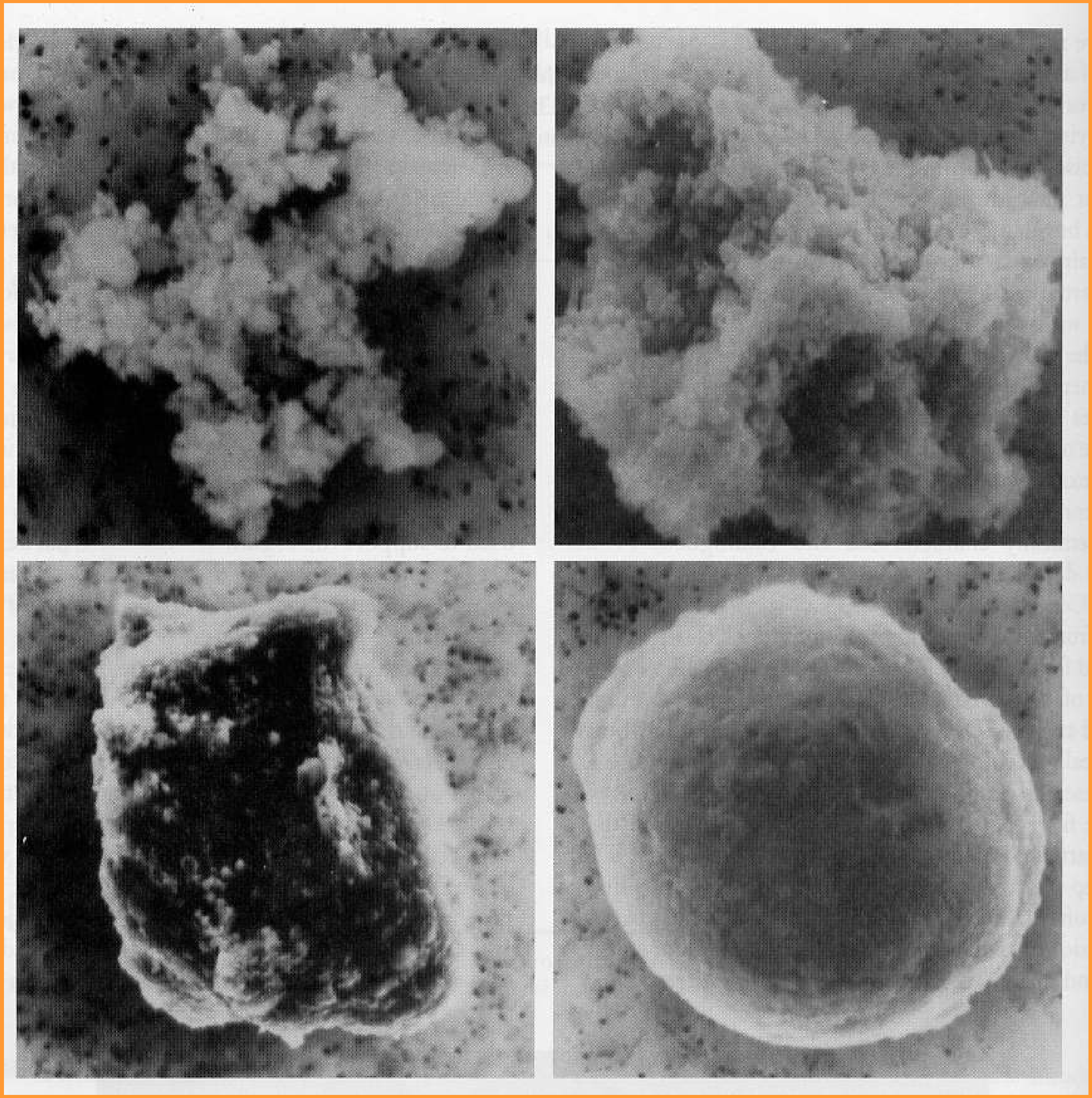

Physico-chemical properties

- Composition: IDPs similar to chondrites for lighter stony elements, but enriched in rare earth elements
- Sizes: power laws with similar exponent
- Radial distribution: double peak distribution
  - Core population peaks at Sun
  - Distant population peaks in asteroid belt
  - ➔ two sources for IPDs:
    - Comets (dust release by nucleus)
    - Asteroids (collisions)

TABLE III
Average Elemental Composition (All Major and Selected Minor and Trace Elements) of Several Chondritic IDPs Is Compared with C1 Chondrite Composition[a]

Element	C1	IDP	Variation	T_c
Mg	1,071,000	0.9	0.6–1.1	1067
Si	1,000,000	1.2	0.8–1.7	1311
Fe	900,000	1	1	1336
S	515,000	0.8	0.6–1.1	648
Al	84,900	1.4	0.8–2.3	1650
Ca	61,100	0.4	0.3–0.6	1518
Ni	49,300	1.3	1.0–1.7	1354
Cr	13,500	1.1	0.9–1.4	1277
Mn	9,550	1.1	0.8–1.6	1190
Cl	5,240	3.6	2.8–4.6	863
K	3,770	2.2	2.0–2.5	1000
Ti	2,400	1.5	1.3–1.7	1549
Co	2,250	1.9	1.2–2.9	1351
Zn	1,260	1.4	1.1–1.8	660
Cu	522	2.8	1.9–4.2	1037
Ge	119	2.3	1.6–3.4	825
Se	62	2.2	1.6–3.0	684
Ga	38	2.9	2.1–3.9	918
Br	12	34	23–50	690

[a] The IDP abundances are normalized to iron (Fe) and to C1. C1 abundance is normalized to Si = 1,000,000 condensation temperatures T_c (°C). From E. K. Jessberger *et al.* (1992). *Earth Planet. Sci. Lett.* **112**, 91–99.

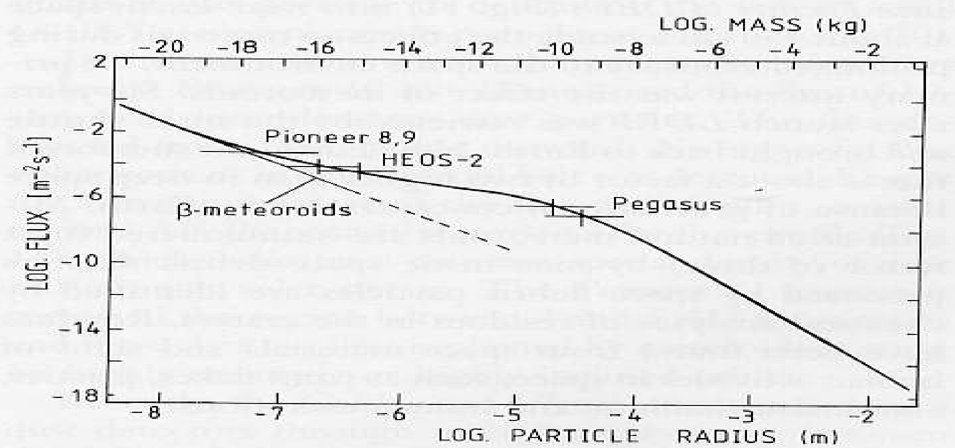

FIGURE 10 Cumulative flux of interplanetary meteoroids on a spinning flat plate at 1 AU from the Sun. The solid line has been derived from lunar microcrater statistics and it is compared with satellite and spaceprobe measurements.

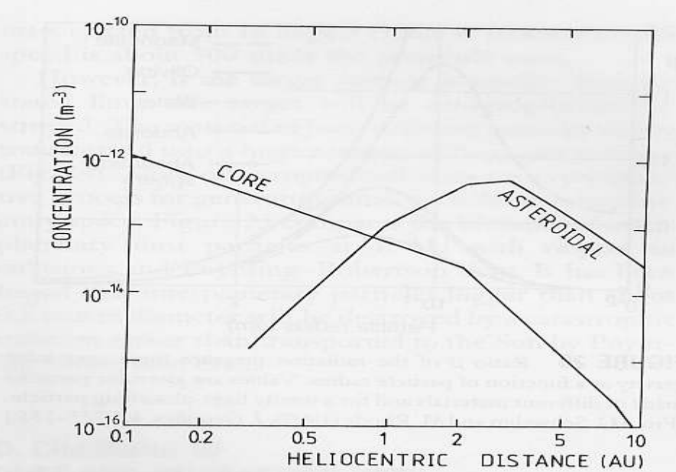

FIGURE 19 Radial dependence of meteoroid concentrations for two main populations in interplanetary space according to Divine (1993). The values given refer to particles with masses $> 10^{-4}$ g. The zodiacal core population comprises particles of all sizes, whereas the asteroidal population comprises only big ($>10^{-6}$ g) particles.

- <u>Lifetime of dust:</u> short lifetime ~ 1000-100000 y
  - Removal effects
    - Poynting-Robertson effect

      (IPDs either blown out of the solar system or spiraling into the Sun
  - Destruction effects
    - Collisions
    - Electrostatic disruption
    - Heating &evaporation
  - Continuous supply necessary!

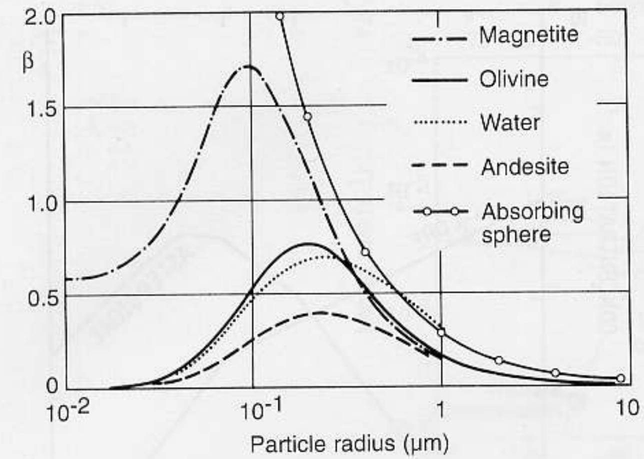

FIGURE 20 Ratio β of the radiation pressure force over solar gravity as a function of particle radius. Values are given for particles made of different materials and for a totally light-absorbing particle. [From G. Schwehm and M. Rhode (1997). *J. Geophys.* **42**, 727–735.]

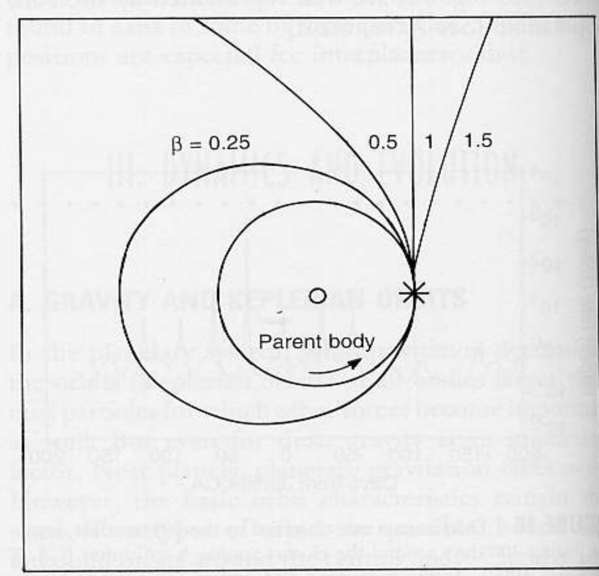

FIGURE 21 Orbits of beta-meteoroids that were generated from a parent body at the position indicated by the asterisk. β values of differently sized fragments are indicated; big β values refer to small particles.

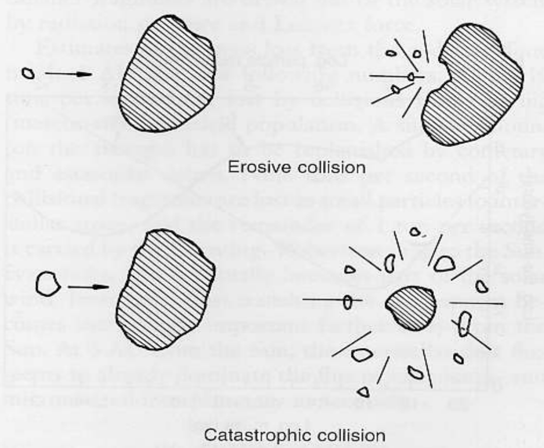

FIGURE 23 Schematics of meteoroid collisions in space. If the projectile is very small compared to the target particle, only a crater is formed in the bigger one. If the projectile exceeds a certain size limit the bigger particle is also shattered into many fragments. The transition from one type to the other is abrupt.